Chemical Composition of Floating and Sunken In-Situ Burn Residues from the Deepwater Horizon Oil Spill

Scott A. Stout[a*] and James R. Payne[b]

[a]NewFields Environmental Forensics Practice, LLC, 300 Ledgewood Pl., Suite 305, Rockland, MA
[b]Payne Environmental Consultants, Inc., 1651 Linda Sue Lane, Encinitas, CA

Abstract

In-situ burning during the *Deepwater Horizon* oil spill generated tens of thousands of barrels of *in-situ* burn (ISB) residues in the northern Gulf of Mexico (GoM), most or all of which eventually sank to the seafloor. Chemical analyses showed floating and sunken (~1400 m deep) ISB residues (1) exhibited distinct *n*-alkanes and UCM profiles inconsistent with vapor-pressure driven evaporation, (2) were relatively enriched in pyrogenic PAHs, particularly less stable (mostly) linear PAH isomers formed during burning, and (3) had lost petroleum biomarkers, relative to their volatility. PAH concentrations in ISB residues indicate between 26,800 and 37,800 kg of total PAHs (TPAH51) and 2880 and 4060 kg of 16 Priority Pollutant PAHs were potentially deposited on the seafloor in discrete ISB residue particles. Despite this additional benthic impact, ISB reduced the total mass loadings of PAH from the burned oil to the GoM by 89% (ignoring any re-deposition from atmospheric emissions).

Keywords

Oil Spill
In-Situ Burning
Hopane
Polycyclic aromatic hydrocarbons
Mass loading

*corresponding author: Tel.: +1 781 681 5040; e-mail: sstout@newfields.com

1. Introduction

In-situ burning of oil spilled on water has been a somewhat controversial oil spill countermeasure in the U.S. for approximately 20 years (Evans, 2001). The controversy stems from environmental concerns over the character and fate of the atmospheric emissions generated and of the unburned oil residue left floating at the burn site. The emissions include combustion gases (CO and CO_2), volatile unburned hydrocarbons, and condensed PAH-laden particulates (soot or black carbon). The unburned oil residue, referred to herein as *in-situ* burn (ISB) residue, is what remains of the floating oil after combustion ceases, i.e., when the heat loss to the water reduces the vaporization rate of the oil below what is necessary to sustain combustion.

Physically, ISB residues are often viscous, sometimes tar-like, and thereby generally similar to severely weathered oil. The density of an ISB residue is expectedly higher than the parent oil, even exceeding the density of water and thereby causing the ISB residue to sink (API, 2002; NOAA, 2014). This sinking behavior was first realized after significant quantities of burn residues sunk following the 1991 *Haven* oil spill and fire (Moller, 1992) and was subsequently confirmed in laboratory experiments for many different oils (Buist et al., 1997). Based upon laboratory experiments, sinking behavior of ISB residues seems favored for heavier oils (fuel oils or heavy crudes) although the real-world behavior of ISB residues from lighter oils, such as the Macondo oil released during the *Deepwater Horizon* (DWH) oil spill, is difficult to predict.

Chemically, ISB residues are often enriched in asphaltenes, resins, and metals that become concentrated as volatile and semi-volatile hydrocarbons are consumed or otherwise lost. Residue may also contain “extra” combustion-derived, or pyrogenic, PAHs that were produced within the oil from either the intense heat radiated back into the slick or as soot particles that condense from the fire’s smoke and re-deposit within the oil residue (Wang et al., 1999; Garrett et al., 2000).

In-situ burning was a widely used countermeasure in response to the DWH oil spill (Figs. 1 and 2). Between April 28 and July 19, 2010, Mabile and Allen (2010) reported approximately 220,000 to 310,000 barrels (bbls) of floating Macondo crude oil were consumed in 411 separate ISB events. Remarkably, this volume of oil consumed is approximately equal to the total volume of oil released during the *Exxon Valdez* oil spill (240,500 bbls; NOAA, 1992). The mass, character, and fate of atmospheric emissions

from these 411 events have been extensively studied (Ryerson et al., 2011; Perring et al., 2011), whereas studies concerning the Macondo oil ISB residues are limited (Shigenaka et al., 2015). The Macondo ISB residues were described as "stiff, taffy-like material" that were estimated to represent only "a few percent of the original volume burned" (Allen, 2011); although no laboratory experiments were conducted to determine the actual burn efficiency(s). Burn efficiency is primarily a function of slick thickness (Fingas, 2011), which undoubtedly varied among the 411 burn events during the DWH oil spill. However, earlier laboratory experiments (Garrett et al., 2000) and our results (see below), suggest the burn efficiency for the *in-situ* burn conducted during DWH response were likely on the order of 85%. Thus, the 411 ISB events (that consumed 220,000 to 310,000 bbls of oil) are estimated to have yielded approximately 38,800 to 54,700 bbls of ISB residue. There was no attempt to mechanically recover the ISB residues, and field observations indicated the ISB residues formed during DWH spill response most likely sank (A. Allen, personal communication, 2014).

In this study, we report on the chemical composition of two floating Macondo oil ISB residues collected immediately following discrete ISB events conducted on May 5 and May 19, 2010. The ISB residues are compared to fresh Macondo oil and to naturally-weathered (unburned) floating Macondo oils collected from the spring and summer of 2010. In addition, the two floating ISB residues are also compared to three discrete, semi-solid oils collected from the deep seafloor approximately 3 km north of the Macondo wellhead, whose compositions indicate they are ISB residues that had sunk to the seafloor.

2. Samples and Methods

2.1 In-Situ Burn Residue Samples

Two floating ISB residue samples were collected prior to cooling and immediately following ISB events that took place on May 5 and May 19, 2010 approximately 10 km south and 17 km northeast from the Macondo wellhead (Fig. 2; Table 1). Several hundred barrels of crude oil were reportedly consumed in both of these events (Table 1). The representativeness of these two ISB residues – among all of the 411 Macondo oil ISB residues produced – is uncertain but given their comparability to one another (see below) they are assumed to be typical of the ISB residues produced.

Three sunken burn residues were collected from the seafloor during the *HOS Sweet Water* 6 NRDA cruise on August 27, 2011 from locations approximately 2.6 km north of the wellhead at water depths of approximately 1,430 m (Fig. 2; Table 1). The samples were collected using an ROV-operated coring device or a "slurp gun" apparatus, both of which were able to capture the visible "lumps" of oil resting on the seafloor (Fig. 3). Upon retrieval, the cores were extruded or the slurp-gun filters removed from their vacuum canisters and the discrete sunken oils collected for analysis (Fig. 3). The three samples exhibited different physical properties as described in Table 1. Observations by one of the authors (JRP) during collection indicated that discrete "lumps" or "flakes" of oil were difficult to see on the seafloor within the narrow field of view (3 to 5 m) along prescribed ROV transects. Further, when they were observed they were difficult to collect using the available equipment mounted on the ROV. Therefore, the few samples collected likely under-represent the true distribution of sunken ISB residue throughout the fallout area.

2.2 Samples Compared to ISB Residues

ISB residue results are compared to unweathered Macondo oil and to naturally-weathered floating Macondo oils collected from the sea surface. The former is represented by the average results of six oil samples collected on May 21, 2010 on the drillship *Discoverer Enterprise* from the riser insertion tube that was receiving oil directly from the well's broken riser tube near the seafloor. Six 2.5L liquid (C_5+) oil samples (Bottles 1 to 5 and 71) were collected in sequence at ambient temperature and pressure, i.e., no attempt was made to preserve any exsolving gas fraction as the oil reached ambient conditions. The floating oil compositions are represented by the average of 62 floating oils collected between May 10 and July 29, 2010, i.e., 20 to 100 days after the DWH spill commenced on April 20, 2010. More details of these samples are found in Stout et al. (2016). Among these 62 naturally-weathered floating oils, three samples that represent minimally, moderately, and severely naturally-weathered states are highlighted herein (sample IDs: JF3-2km-onet-20100616-surf-N143, JF2-4km-surf-0-20100524-N100, and GU-10-02-005-T-003, respectively).

2.3 Sample Preparation

All samples were frozen after collection and sent to Alpha Analytical (Mansfield, MA) following normal chain-of-custody procedures for chemical analysis. Upon receipt at the laboratory all samples were stored in the dark and frozen (-20ºC) prior to sample preparation and instrument analysis.

All ISB residue samples were diluted in dichloromethane (DCM) and then processed through a glass fiber filter and anhydrous Na_2SO_4 to remove any particulates and water, respectively. A 1 ml aliquot of the filtered extract was then spiked with surrogate internal standards (SIS; *o*-terphenyl, *n*-tetracosane-d_{50}, naphthalene-d_8, phenanthrene-d_{10}, benzo[a]pyrene-d_{12}, and 5β(H)-cholane) and response internal surrogates (RIS; 5α-androstane, acenaphthene-d_{10}, chrysene-d_{12}) prior to instrumental analysis. Sample preparation of the floating oils was previously described (Stout et al., 2016). The unweathered Macondo oils (50 mg) were diluted in DCM and a 1 ml aliquot was spiked with SIS and RIS prior to instrumental analysis. No silica-gel cleanup of the sample extracts was performed.

Each analytical batch of authentic samples (n<20) included a procedural blank (PB; 1 ml of DCM), a laboratory control sample (LCS) and LCS duplicate (LCSD), each consisting of 1 ml of DCM spiked with selected hydrocarbons in known concentrations to monitor method accuracy, a NIST 1582 standard reference oil, and one sample duplicate (i.e., a single oil prepared twice) as a measure of precision and reproducibility of the data.

2.4 Instrumental Analysis

All sample extracts were analyzed using a (1) modified EPA Method 8015B and (2) modified EPA Method 8270 as described in the following paragraphs. Additional details of these methods are described elsewhere (Douglas et al., 2015).

Modified EPA Method 8015B was conducted via gas chromatography-flame ionization detection (GC-FID; Agilent 6890) equipped with a Restek Rtx-5 (60m x 0.25 mm ID, 0.25 μm film) fused silica capillary column. Extracts were injected (1 μl, pulsed splitless) into the GC programmed from 40°C (1 min) and ramped at 6°C/min to 315°C (30 min) using H_2 (~1 ml/min) as the carrier gas. This analysis was used to determine the concentrations of GC-amenable total extractable material (TEM; C_9-C_{44}) and individual *n*-alkanes (C_9-C_{40}) and (C_{15}-C_{20}) acyclic isoprenoids. Prior to sample analysis a minimum five-point calibration was performed to demonstrate the linear range of the

analysis. The calibration solution was composed of selected aliphatic hydrocarbons within the *n*-C_9 to *n*-C_{40} range. Analyte concentrations in the standard solutions ranged from 1 ng/µl to 200 ng/µl. Target analytes that were not in the calibration solution had the average response factor (RF) of the nearest eluting compound(s) assigned as follows: RF of *n*-C_{14} assigned to C_{15} isoprenoids, *n*-C_{15} assigned to C_{16} isoprenoids; *n*-C_{17} assigned to nor-pristane, and *n*-C_{40} assigned to *n*-C_{39}. All calibration solution compounds that fall within the window were used to generate the average RF for TEM. TEM was quantified by integrating the total C_9-C_{44} area after blank subtraction. Calibration check standards representative of the mid-level of the initial calibration and the PB were analyzed every 10 samples. The check standard's response was compared versus the average RF of the respective analytes contained in the initial calibration. All authentic samples and quality control samples were bracketed by passing mid-check standards.

Modified EPA Method 8270 was conducted via gas chromatography-mass spectrometry (GC-MS; Agilent 7890 GC with 5975c MS) with the MS operated in the selected ion monitoring (SIM) mode for improved sensitivity. Extracts were injected (1 µl, pulsed splitless) into the GC containing a 60m x 0.25 mm ID, 0.25 µm film, Phenomenex ZB-5 capillary column and the oven programmed from 35°C (1 min) and ramped at 6°C/min to 315°C (30 min) using He as the carrier gas. This analysis was used to determine the concentrations of 62 parent and alkylated decalins, polycyclic aromatic hydrocarbons (PAH), sulfur-containing aromatics and 54 petroleum biomarkers (i.e., tricyclic and pentacyclic triterpanes and steranes, and triaromatic steroids). Prior to sample analysis, the GC-MS was tuned with perfluorotributylamine (PFTBA) at the beginning of each analytical sequence. A minimum 5-point initial calibration consisting of selected target compounds was established to demonstrate the linear range of the analysis. Analyte concentrations in the standard solutions ranged from 0.01 ng/µL to 20.0 ng/µL for PAHs and 0.01 ng/µL to 10.0 ng/µL for biomarkers. Quantification of target compounds was performed by the method of internal standards using average response factor (RF) determined in the 5-point initial calibration. Alkylated PAHs were quantified using the RF of the corresponding parent, triterpanes were quantified using the RF's for 17α(H),21β(H)-hopane, and steranes and triaromatic steroids were quantified using the RF of 5β(H)-cholane. Biomarker identifications were based upon comparison to selected authentic standards (*Chiron Laboratories*), elution patterns in the peer-reviewed

literature, and mass spectral interpretation from full scan GC/MS analyses conducted in our laboratory.

Aliquots of each sample extract were used to determine the gravimetric weight of the recoverable oil, thereby allowing the concentrations of target analytes to be reported on an oil weight basis ($\mu g/g_{oil}$). All sample locations and surrogate-corrected concentration data are publically available through NOAA Deepwater Horizon NRDA data portal, DIVER (Data Integration Visualization Exploration and Reporting), available at https://dwhdiver.orr.noaa.gov/. All concentrations reported herein have been converted to non-surrogate values.

2.5 Degree of Weathering Quantification

The degree of weathering in each ISB residues (and floating oils) was determined based upon mass losses relative to the conservative internal marker within the oil, *viz.*, 17α(H),21β(H)-hopane (hopane), which has proven recalcitrant to biodegradation (Prince et al., 1994) and photo-oxidation (Garrett et al., 1998). The percent depletion of any given fraction (e.g., TEM or total PAHs) or individual chemical (e.g., naphthalene) in the ISB residues (and floating oils) was estimated using the following formula:

$$\%\text{Depletion of A} = [((A_0/H_0) - (A_s/H_s))/(A_0/H_0)] \times 100 \qquad \textit{Eq. (1)}$$

where A_s and H_s are the concentrations of the target analyte and hopane in the ISB residue (or floating oil) sample, respectively, and A_0 and H_0 are the concentrations of the target analyte and hopane in the average, fresh Macondo source oil. Although hopane can be removed under some circumstances, if it (H_S) were removed in a given sample, any % depletions calculated would be underestimated and % enrichments (i.e., negative % depletions) would be overestimated.

3. Results and Discussion

3.1 Overall Character of Floating ISB Residues

Figure 4 shows the GC/FID chromatograms for fresh Macondo oil and the two floating ISB residues. The fresh oil is dominated by *n*-alkanes that span from *n*-C_8 to *n*-C_{40} with decreasing abundance with increasing carbon number (Fig. 4A). The prominence of the

resolved *n*-alkanes results in only a small unresolved complex mixture (UCM), as is typical of unweathered crude oil. Each of the ISB residues has lost a substantial proportion of the more volatile compounds toward the left of each chromatogram (Fig. 4B-C). As a consequence most of the mass of the ISB residues occurs within the prominent UCM, which exhibits a distinctive shape that gradually rises from about *n*-C_{13} to a maximum at *n*-C_{34}, before quickly dropping off (due to chromatographic conditions; Fig. 4B-C).

The TEM (C_9 to C_{44}) concentrations and mass losses (relative to fresh Macondo oil) for the floating ISB residues are indicated on Figure 4 (calculated from Eq. 1; TEM concentrations are from Table 2). Both ISB residues experienced a loss of nearly two-thirds the C_9-C_{44} mass compared to fresh Macondo oil (67 and 63%). Simulated distillation of the fresh Macondo oil had indicated approximately 20% of the oil's C_5+ mass occurred in the C_5 to C_9 range (Stout et al., 2016). Thus, it can be concluded that the floating ISB residues studied had experienced a total C_5+ mass loss of approximately 85% (83 to 87%), which reasonably reflects the burn efficiency achieved in these particular ISB events. This percentage is typical of efficiencies achieved in other *in-situ* burns of light crude oil (Garrett et al., 2000).

Losses of the more volatile compounds in the Macondo oil are expected in the ISB residues, which undoubtedly experienced evaporation before, during, and perhaps even after the ISB events. However, there are some peculiarities evident in the ISB residues' boiling distributions that become evident when they are compared to naturally-weathered floating oils that had experienced no 'extra' heating associated with *in-situ* burning. That is, the mass losses from the floating ISB residues do not appear to be entirely attributable to evaporation.

Toward this end, a population of 62 floating Macondo oils collected in the spring and summer of 2010 demonstrated that the floating (unburned) oils had experienced a wide range in weathering caused by variable degrees of dissolution of lower-molecular-weight components during the oil's rise through the water-column followed by predominant evaporation after reaching the surface, although photo-oxidation of some susceptible compounds had also occurred (Stout et al., 2016). The variability among naturally-weathered (unburned) floating Macondo oil is demonstrated upon inspection of the

GC/FID chromatograms for representatives of minimally, moderately, and severely weathered (unburned) floating Macondo oils (Fig. 5A-C). These chromatograms show the predictable decrease in *n*-alkanes (and other compounds) with increasing vapor pressure (right to left) and the corresponding decrease in the lower boiling portion of the UCM. Such patterns are entirely consistent with evaporation losses.

For comparison, the GC/FID chromatograms for the two floating ISB residues (from Fig. 4B-C) are shown again in Fig. 5D and 5E on the same approximate vertical scale as for the naturally-weathered floating oils (e.g., the UCM maximum at *n*-C_{34} is about the same height in each chromatogram). Inspection reveals that the ISB residues' chromatograms exhibit different *n*-alkane profiles than the naturally evaporated floating oils. Specifically, the ISB residues exhibit a greater retention of some of the more volatile *n*-alkanes (*n*-C_{14} to *n*-C_{18} or so) and a greater loss of some of the less volatile *n*-alkanes (*n*-C_{19} to *n*-C_{30}) relative to the UCM. In addition, the shape of the UCMs for the naturally evaporated floating oils do not exhibit the same gradual rise from *n*-C_{12} to *n*-C_{34} that the ISB residues exhibit (Fig. 5B-C and Fig. 5D-E). Instead, the naturally weathered floating oils' UCMs tend to rise more sharply at their front ends and then remain mostly level as they approach *n*-C_{34} (Fig. 5B-C). The distinct shapes of *n*-alkane and UCM profiles for the ISB residues indicate that they have experienced losses that are different from the natural evaporation experienced by unburned floating oil. This will be discussed further below.

3.2 Overall Character of Sunken Burn Residues

The distinctive chromatographic features of the floating ISB residues described above (Fig. 4B-C) are also evident in two of the samples collected from the deep-seafloor, which we believe confirms their origin as sunken burn residues (Fig. 6A-B). The sunken burn residues #82 and #83 both also exhibit decreasing losses of *n*-alkanes with increasing carbon number and UCM's that gradually rise from around *n*-C_{12} to a maximum at *n*-C_{34} (Fig. 6A-B). In fact, the burn residue #82 sample's UCM appears somewhat concave indicating an even greater loss of unresolved compounds in this sample.

The GC/FID chromatogram for the third sunken burn residue (#76) is distinct from the others and is dominated by *n*-alkanes and a prominent UCM in the "diesel-range"

(*n*-C_{10} to *n*-C_{25}). No known weathering process of crude oil could produce the prominent diesel-range UCM, which thereby indicates that this particular burn residue contains a mixture of a diesel-like petroleum and a crude oil. The presence of a mixture renders this sample difficult to directly compare to the other sunken burn residues, but as will be shown below (Table 2), this sample clearly contains elevated pyrogenic high molecular weight (4- to 6-ring) PAHs consistent with it being comprised of some sort of burn residue. The mechanism by which a mixture of diesel-like petroleum and burned crude oil ended up on the seafloor as a discrete "flake" of oil (Fig. 3D) is uncertain. We hypothesize this sample may be derived from the original rig explosion and fire, in which some uncombusted diesel fuel may also have been retained in a sunken residue or perhaps an uncombusted residue of the diesel gel used to ignite floating oils during the *in-situ* burning operations (A. Allen, personal communication, 2014). Based on biomarker characterizations, however, the non-diesel, higher-molecular-weight fraction of sample #76 is unquestionably derived from Macondo oil.

The TEM (C_9 to C_{44}) concentrations and mass losses (Eq. 1) for the sunken burn residues are indicated in Figure 6. The #82 and #83 residues experienced higher (73%) and lower (58%) TEM mass depletions than the floating ISB residues (Fig. 4) likely suggesting some variability in the burn efficiencies achieved in generating these particular sunken burn residues. Considering approximately 20% of the fresh Macondo oil's mass occurred below C_5 (Stout et al., 2016), the burn efficiency suggested by these two sunken residues was 78 and 93%, which bracket the range of the floating ISB residues (83 and 87%; see above). Thus, we believe the 85% burn efficiency is a reasonable estimate for the ISB events during the DWH oil spill. The TEM mass "loss" from the atypical #76 burn residue is -13% due to the confounding influence of the "extra" distillate component in this sample (which increased the TEM and decreased the hopane concentration in this sample).

3.3 Naturally-Evaporated Oil versus Burn Residues

The different *n*-alkane profiles evident between the floating or sunken burn residues and naturally-evaporated floating Macondo oil (described above; Fig. 5 and 6) are more clearly shown in Figure 7. Fig. 7A shows the percent depletion for *n*-alkanes and selected acyclic isoprenoids between *n*-C_9 and *n*-C_{30} in the floating ISB residues versus that for severely evaporated (unburned) floating Macondo oil. Both of the floating ISB

residues have lower percent depletions for *n*-alkanes between *n*-C_{13} and *n*-C_{18} and higher percent depletions for *n*-alkanes between *n*-C_{19} and *n*-C_{30} than severely evaporated floating oil (Fig. 7A).

Figure 7B compares the percent depletions for alkanes in the sunken burn residues (#82 and #83) compared to severely evaporated (unburned) floating Macondo oil. The #83 burn residue exhibits lower percent depletions for *n*-alkanes between *n*-C_{13} and *n*-C_{18} and higher percent depletions for *n*-alkanes between *n*-C_{19} and *n*-C_{30} than naturally-evaporated floating oil. The #82 burn residue exhibits higher percent depletions for *n*-alkanes between *n*-C_{17} and *n*-C_{30} (Fig. 7B). (The #76 sunken burn residue flake is not shown due to the confounding influence of the "extra" diesel-range *n*-alkanes and "dilution" of hopane due to the diesel-like petroleum present in this sample; Fig. 6C).

The loss of *n*-alkanes due to natural evaporation, which is driven only by vapor pressure of the *n*-alkanes, would not produce the "extra" *n*-alkanes below *n*-C_{18} and "depleted" *n*-alkanes above *n*-C_{19} that are evident in the floating and sunken burn residues (Fig. 7). This indicates that simple vapor pressure-driven evaporation is not the only process that has affected the ISB residues. Biodegradation, which can preferentially deplete *n*-alkanes, is unlikely for the floating ISB residues that were collected immediately after the ISB events ceased. Furthermore, the percent depletion for acyclic isoprenoids (e.g., pristane and phytane) are comparable in the floating ISB residues to corresponding *n*-alkanes (*n*-C_{17} and *n*-C_{18}; Fig. 7A), indicating evaporation, not biodegradation, is responsible in the floating ISB residues. Some minor biodegradation of *n*-alkanes in the sunken burn residue #83 is indicated, however (Fig. 7B) but is insufficient to explain the loss of long-chain *n*-alkanes up to *n*-C_{30}. Therefore, an alternative explanation must exist.

We hypothesize that the burn residues' unusual *n*-alkane (and UCM) profile(s) may be a function of relative ignitability *versus* volatility of *n*-alkanes (and other homologous hydrocarbon series "buried" within the UCM). Specifically, the ignition temperatures for *n*-alkanes (and other homologues) reportedly *decrease* with increasing carbon number whereas the boiling points of *n*-alkanes (i.e., the temperature at which evaporation will occur) *increase* with increasing carbon number (Stauffer et al., 2008; Merker et al.,

2012). For example, the ignition temperature for *n*-C_{10} (206ºC) is higher than that of *n*-C_{20} (143ºC), which in turn is higher than that of *n*-C_{30} (112ºC; Shimy 1970). On the other hand, the boiling point of *n*-C_{10} (174ºC) is lower than that of *n*-C_{20} (343ºC), which in turn is lower than that of *n*-C_{30} (450ºC). Relatedly, the cetane number of *n*-alkanes also increases with carbon chain length (Merker et al., 2012). The cetane number is a relative metric used by fuel scientists to quantify how quickly a single compound or fuel ignites inside compression ignition engines; the higher the cetane number, the shorter the time to ignition inside an engine (Merker et al., 2012). Combustion within an engine may, in terms of its effect on *n*-alkanes, mimic combustion within an *in-situ* burn. Therefore, we hypothesize that the temperature(s) achieved during *in-situ* burning had varying effect(s) on the processes of evaporation (controlled by boiling point) and combustion (controlled by ignition temperature) of *n*-alkanes (and other homologues). The preferential and more rapid combustion of the *n*-C_{19} to *n*-C_{30} *n*-alkanes (and other homologues in the UCM) could have resulted in the distinct *n*-alkane (and UCM) profiles observed (Fig. 7). Thus, the ISB residue *n*-alkane (and UCM) profiles are distinguishable from those achieved by natural (vapor pressure-driven) evaporation experienced by the floating (unburned) Macondo oils. This difference should allow for the distinction between ISB residues and naturally-weathered oil residues following an oil spill in which *in-situ* burning was employed.

3.4 PAH Concentrations and Distributions in Burn Residues

The concentrations of PAHs and hopane in the floating and sunken burn residues are given in Table 2. The average concentrations of these analytes in fresh and naturally-weathered (unburned) floating oils are also given for comparison. Figure 8 shows these data plotted as hopane-normalized histograms that allows for a visual comparison among the samples. The histogram for the "diesel-bearing" burn residue (#76) is not shown due to the confounding influences of the distillate fraction on the PAH and hopane concentrations in the crude oil fraction of this residue. However, inspection of Table 2 reveals the elevated concentrations of many of the higher molecular weight (4- to 6-ring) PAHs indicative of combustion in this sample, suggesting it is indeed comprised of some sort of burn residue that is mixed with an unburned distillate product.

Inspection of Figure 8A-B shows that the PAH distributions in two floating ISB residues studied are quite similar to one another. The major PAH homologue groups in both of

these are reduced compared to fresh Macondo oil indicating the ISB residues experienced a reduction of *most* PAHs. However, upon comparison to the average composition of unburned floating oils, it can be seen that, on average, the floating ISB residues had experienced a greater reduction among lower molecular weight PAHs (LPAH: 2- and 3-rings; N0 through BF in Fig. 8) than unburned floating oils. The relative abundance of higher molecular weight PAHs (HPAH: 4- to 6-rings) in the ISB residues appear to be comparable or slightly higher than is present on average in the unburned floating oils (FL0 through GHI in Fig. 8A-B). This suggests that *in-situ* burning of floating crude oil reduces the concentrations of LPAHs to a greater extent than natural weathering processes (e.g., evaporation, dissolution, photo-oxidation). Although some reduction in HPAHs in the unburned floating oils was attributed to photo-oxidation (e.g., BC3 and BC4; Fig. 8A-B; Stout et al. 2016), this process apparently did not affect the ISB residues (likely because they were collected immediately after the ISB events).

The two sunken burn residues studied exhibit more variable PAH distributions than the floating ISB residues (Fig. 8C-D). Again, however, both of the sunken ISB residues had experienced a greater relative loss of LPAHs than HPAHs with the overall losses from the #82 burn residue exceeding those of the #83 burn residue. This suggests that the degree of LPAH losses was not necessarily uniform among floating ISB residues before the residues sank, which suggests that the burn efficiencies of all 411 ISB events were not uniform. Both of the sunken burn residues still retain some naphthalenes (Fig. 8C-D; Table 2), which indicates that they sank before experiencing severe evaporation after the fire was extinguished (e.g., severely evaporated unburned floating oil contains virtually no naphthalenes; Table 2.).

Most notably, both sunken burn residue samples contain some HPAHs whose relative abundances (and absolute concentrations; Table 2) markedly exceed those of the average unburned floating oils, and for some PAHs, even exceed those of the fresh Macondo oil (Fig. 8C-D). This increase is most evident among the Priority Pollutant HPAHs that are long-recognized as combustion-derived PAHs (Hites et al., 1977). For example, the #83 burn residue clearly contains excess relative abundances of fluoranthene, pyrene, benz(*a*)anthracene, and numerous 5- and 6-ring PAHs (Fig. 8D). The absolute concentrations of most of these HPAHs are also higher in the floating and sunken burn residues than in either the fresh Macondo oil or naturally weathered

(unburned) floating Macondo oils (see bolded values in Table 2). This is explored further in the next section.

3.5 PAH Enrichment in Burn Residues

The apparent enrichment of PAHs can be quantified by calculating the percent depletion relative to hopane (negative depletion equals enrichment) using the concentrations in Table 2 and Eq. 1.

For comparison to the burn residues, the percent depletions of PAHs for severely weathered (unburned) floating oil are shown in Fig. 9A. This (unburned) floating oil shows percent depletions approaching 100% for most PAH analytes, with no analytes showing any enrichment (Fig. 9A). The losses of PAHs in floating oil were brought about by the combined effects of natural weathering processes, *viz*., dissolution, evaporation, and photo-oxidation (Stout et al., 2016). Dissolution and more importantly, evaporation, were recognized as the dominant processes that depleted LPAHs (N0-DBT4), which results in slightly lower percent depletions with increasing degree of alkylation among homologue groups within this range. However, photo-oxidation is considered responsible for depletion among HPAHs (FL0-GHI; Stout et al., 2016) as evident in the higher percent depletions with increasing alkylation among naphthobenzothiophene (NBT) and benz(*a*)anthracene/chrysene (BC) homologues and greater depletion of benz(*a*)anthracene (BA0) over its isomer, chrysene (C0) (Fig. 9A; e.g., Garrett et al., 1998; Lee, 2003; Plata et al., 2008). See Stout et al. (2016) for additional discussion on the natural weathering of the floating Macondo oils.

The ISB residues studied herein also exhibit losses of most PAHs, with the highest percent depletions being evident among lower molecular weight PAHs wherein the extent of depletion decreases with increasing degree of alkylation within each homologue group (Fig. 9B-E). These depletions appear consistent with losses attributable to dissolution and evaporation, which more greatly effect lower molecular weight PAHs and less alkylated homologues. We can only speculate as to how much of these losses occurred prior to, during, or after the burn events. However, given that highly weathered floating oils, particularly those that had formed emulsions, are typically poor candidates for *in-situ* burning owing to the difficulty of sustaining a burn in such oils (Walavalkar, 2001), the ISB residues studied were more likely generated from floating oil

slicks that were not yet excessively weathered/emulsified. Supporting this likelihood is the lack of evidence that photo-oxidation contributed to depletion of PAHs in the ISB residues, *viz.*, none of them exhibit the atypical homologue pattern among naphthobenzothiophenes or benz(*a*)anthracenes/chrysenes evident in naturally-weathered floating oil.

However, all four burn residues clearly exhibit percent enrichments (i.e., negative percent depletions) among several PAHs conventionally considered to be combustion-derived (i.e., pyrogenic) ranging from fluoranthene (F0) to benzo(*g,h,i*)perylene (GHI) that can only reasonably be attributed to the formation of these PAHs during the ISB events (Fig. 9B-E). As can be seen, naphthalene and the other lower molecular weight PAHs are mostly depleted in the ISB residues, while acenaphthylene (AY) and anthracene (A0) are minimally depleted or enriched. Among higher molecular weight PAHs the ISB residues exhibit enrichments among fluoranthene (FL0), pyrene (PY0), benz(*a*)anthracene (BA0) and all of the 5- and 6-ring PAHs (BBF through GHI). Benzo(*j/k*)fluoranthene (BJKF) exhibits the largest enrichments (approximately 4.5- to 29-times higher in the ISB residues than in fresh Macondo oil) although it is acknowledged that the absolute percent enrichment for some of these high molecular weight PAHs may be exaggerated due to these compounds' very low concentrations in the fresh oil (< 1 μg/g; Table 2). Nonetheless, the systematic enrichment of acenaphthylene, anthracene, fluoranthene, pyrene, benz(*a*)anthracene and all of the 5- and 6-ring PAHs in the floating and sunken ISB residues is clearly evident relative to fresh Macondo oil (Fig. 9B-E), and to highly weathered floating Macondo oil (Fig. 9A).

The enrichment of these particular PAHs in the burn residues cannot be attributed solely to any concentrating effect the fire had on the original oil (i.e. reduction in overall oil mass). If it were, then the other high molecular weight PAHs (e.g., alkylated naphthobenzothiophenes and benz(*a*)anthracenes/chrysenes) would be similarly enriched – yet they are not (Fig. 9B-E). Therefore, the percent enrichments evident in the ISB residues must be due to the formation of these PAHs during *in-situ* burning of the Macondo oil. As observed and concluded in earlier studies of ISB residues (Wang et al., 1999; Garrett et al., 2000), these "extra" PAHs were likely formed by intense heating within the burning oil itself or reflect the contribution from PAH-rich soot particles that

were emitted from the fire, condensed within the fire's smoke and were then re-deposited within the unburned floating ISB residue.

Further evidence for the formation of these high molecular weight PAHs can be seen upon inspection of partial GC/MS extracted ion profiles (EIPs) for representative molecular ions. Figure 10A shows the partial *m/z* 202 EIP that shows the increase in fluoranthene and pyrene in the #2 floating and #83 sunken ISB residues. There is a clear increase in the magnitude of both these peaks relative to an unidentified compound with the same approximate boiling point (i.e., see peak with asterisk; Fig. 10A) reflecting the enrichments of fluoranthene and pyrene in the burn residues (Fig. 10A). Notably the formation of the fluoranthene isomer appears to have been preferred over the pyrene isomer. Anthracene was also preferentially formed over phenanthrene, as indicated in the former's higher percent enrichments (Fig. 9). Similarly, benz(*a*)anthracene isomer was preferentially formed over chrysene isomer in the burn residues (Fig. 10B). This is notable because benz(*a*)anthracene was preferentially depleted relative to chrysene in floating oils (Fig. 9A), which (as described above) was attributed to the former's greater susceptibility to photo-oxidation (Stout et al., 2016). Finally, there were marked increases evident in the abundances of benzo(*j/k*)fluoranthene, benzo(*a*)fluoranthene, and benzo(*a*)pyrene isomers relative to benzo(*b*)fluoranthene and benzo(e)pyrene in ISB residues (Fig. 10C). The preferential formation of less stable linear (or mostly linear) PAH isomers over others (e.g., anthracene over phenanthrene, fluoranthene over pyrene and benz(*a*)anthracene over chrysene) is consistent with the rapid, high temperature heating and the relatively rapid quenching reactions associated with combustion (e.g., Budzinski et al. 1997; Dickhut et al. 2000; Yunker et al. 2002). Comparable relationships in the preferential formation of certain PAH isomers have been observed in previously-studied ISB residues (Wang et al., 1999; Garrett et al., 2000).

3.6 Effect of In-Situ Burning on Biomarkers

The concentrations of targeted biomarkers – terpanes, steranes, and triaromatic steroids – detected in the ISB residues and fresh Macondo oil are given in Table 3. Biomarkers are conventionally considered relatively resistant to most natural weathering and therefore are commonly used in identifying spilled oils to their source (e.g., Wang et al., 2006). Comparison of the GC/MS extracted ion profiles (EIPs) of the various biomarkers in the ISB residues studied revealed – as might be anticipated – that they were highly

consistent with the unweathered Macondo oil. For example, Fig. 11 shows the partial *m/z* 191 EIPs for fresh Macondo oil and the floating ISB residue #2 are qualitatively comparable. Other EIPs representing dia- and regular steranes and triaromatic steroids (TAS) are equally comparable (not shown). Thus, qualitatively the distributions of biomarkers do not appear to have been affected by the *in-situ* burning of the oil.

However, when the concentration data for the individual biomarkers (Table 3) are evaluated for their percent depletions relative to hopane (Eq. 1) it becomes clear that some biomarkers were affected by *in-situ* burning. These effects were consistent among all four of the ISB residues studied and are exemplified in Fig. 11C for the floating ISB residue #2, which shows a relationship exists between the percent depletion relative to hopane and the relative retention time (RRT) of the biomarker. RRT is essentially a measure of the compound's volatility and is based on the retention times of *n*-alkanes under the same GC/MS conditions. For example, *n*-C_{24} has an RRT of 2400, etc. There is an overall trend wherein the percent depletion of biomarkers increases with greater volatility (lower RRT). In each of the ISB residues there was a loss of tricyclic terpanes relative to hopane, and an increase in C_{31} to C_{35} homohopanes relative to hopane (Fig. 11C). This trend indicates that there was some loss of hopane, and less volatile terpanes, likely caused by *in-situ* burning. As such, the calculated percent depletions or enrichments of PAHs relative to hopane plotted in Figure 9 are somewhat under- or over-estimated, respectively, but nonetheless reveal the enrichment of pyrogenic PAH in ISB residues. Similarly, dia- and regular steranes were also depleted and, acknowledging some scatter due to low concentrations, fall along the same trend as the terpanes (Fig. 11C). We attribute the trend in terpanes and steranes to vaporization and/or combustion of these normally recalcitrant biomarkers during *in-situ* burning. This loss is not unexpected given that there also were depletions among high boiling *n*-alkanes (Fig. 7).

The TAS are also depleted in the ISB residues but, as exemplified in Fig. 11C, these compounds' tend to exhibit greater percent depletion than can be explained by their volatility. For example, despite having RRTs between trisnorhopane (T12) and hopane (T19), all four TAS measured exhibit percent depletions about 20% higher than these terpanes (Fig. 11C). We attribute this additional ~20% depletion of TAS in the ISB residues to photo-oxidation of the TAS in the floating oils prior to *in-situ* burning.

Previous studies of floating Macondo oil have demonstrated the susceptibility of the TAS to photo-oxidation, which rapidly affected floating Macondo oil under the conditions of the DWH oil spill (Aeppli et al., 2014; Stout et al., 2016).

3.7 PAH Mass Loading due to In-Situ Burning

Given the increased concentrations and relative enrichments of most pyrogenic PAHs in the burn residues studied, it is appropriate to consider the effect that *in-situ* burning of oil during the DWH oil spill may have had on PAH mass loading to the GoM surface waters and benthos.

A previous study had estimated $1.35 \pm 0.72 \times 10^6$ kg of soot and aerosols were generated and released into the atmosphere from the 411 ISB events (Perring et al., 2011). At least some fraction of this was redeposited on the sea surface due to particle settling (Fig. 1) and/or carried by precipitation; however, our study cannot further address any mass loading to the GoM associated with this fraction. Our study does provide insight to the PAH mass loading associated with the ISB residues that remained in the water after the 411 ISB events.

As described above, approximately 220,000 to 310,000 barrels (bbls) of floating Macondo crude oil reportedly were consumed in 411 separate ISB events (Mabile and Allen 2010). The TEM-based mass depletions calculated for the floating and sunken ISB residues studied suggested burn efficiencies on the order of 85% were achieved (see above), which is consistent with other studies (Garrett et al., 2000). Back-calculating from the reported volumes consumed (Mibale and Allen, 2010), an 85% burn efficiency would indicate that a total between approximately 38,800 and 54,700 bbl of ISB residue was generated from the 411 ISB events. No effort was made to collect these residues and it is assumed they ultimately sunk (A. Allen, personal communication, 2014), which is supported by our observation of ISB residues on the seafloor. Thus, we estimate that between 38,800 and 54,700 bbl of ISB residues were ultimately deposited on the seafloor, probably as discrete, dispersed particles as shown in Fig. 3. These particles were likely dispersed by subsea currents and spread over much of the seafloor but generally below the areas where *in-situ* burning had occurred (Fig. 2). Our data shows these sinking particles contained PAHs and other hydrocarbons, which otherwise would not have reached the seafloor if *in-situ* burning

had not taken place. These sunken ISB particles thereby additionally exposed benthic resources to these hydrocarbon-bearing particles.

The total mass of PAHs deposited on the seafloor as discrete ISB residue particles can be estimated based the concentrations of PAHs measured in the ISB residues (Table 2) – and an assumed density for the sunken ISB particles (which is necessary to convert the barrels of ISB residue to a mass). Table 4 shows the mass of each PAH analyte per barrel of the four ISB residues studied herein. There was some variability in the mass of PAH among the four ISB residues studied, with the floating ISB residue #2 containing about one third the mass of PAH of the sunken ISB residue #83 (Table 4). The average of all four ISB residues are used to estimate the range in total mass loadings using the minimum (38,800 bbl) and maximum (54,700 bbl) volumes of ISB residues produced from the 411 *in-situ* burn events (Table 4, right hand columns). These calculations show that between approximately 26,800 and 37,800 kg of total PAHs (TPAH51), including 2,880 and 4,060 kg of the 16 Priority Pollutant PAHs (TPAH16) were potentially deposited on the seafloor within discrete ISB residue particles.

The environmental impacts of the aforementioned releases of soot and aerosols to the atmosphere (Perring et al., 2011) and the sinking of ISB residues to the seafloor (Table 4) are undoubtedly significant; however, the overall environmental consequences of *in-situ* burning must also consider the reduction in total mass loadings of oil to GoM surface water (and ultimately to some degree, shorelines) resulting from the *in-situ* burning performed in response to the DWH oil spill.

The results of this comparison are given in Table 5 wherein the average composition of naturally-weathered floating Macondo oil from Table 2 is used to represent the mass loadings of PAH to the GoM surface water if *in-situ* burning had not occurred. As can be seen, if the approximately 258,800 to 364,700 bbl of floating Macondo oil that was subjected to *in-situ* burning had not been burned, a total of approximately 242,000 to 340,000 kg of total PAH (TPAH51) and 15,000 to 21,100 kg of Priority Pollutant PAH (TPAH16) would have remained within surface slicks, perhaps ultimately reaching shorelines. However, on average, *in-situ* burning reduced the total PAH load to the GoM surface water to between approximately 26,800 and 37,800 kg. This mass represents an 89 percent reduction compared to the total PAH load that would have been added if the 258,800 to 364,700 bbl of oil had not been burned (Table 5). Thus, overall *in-situ*

burning significantly reduced the total loading of PAHs to the Gulf of Mexico (ignoring any re-deposition of soot and aerosols from the emissions).

Most individual PAH analytes experienced mass reductions between 80 and 90 percent (Table 5). Numerous pyrogenic PAHs that were recognized to have been generated during the *in-situ* burning process (Fig. 9; see above) still exhibit total net reductions relative to the unburned floating oil. For example, acenaphthylene, anthracene, pyrene, benz(*a*)anthracene, benzo(*b*)fluoranthene, benzo(*e*)pyrene, and dibenz(*a,h*)anthracene each exhibit overall reductions (44, 41, 20, 19, 52, 64, and 46%, respectively) despite being generated. These percent reductions are simply lower than other PAHs not generated during *in-situ* burning (Table 5).

Only six PAHs exhibited overall increases (i.e., negative reductions) in the mass loadings caused by *in-situ* burning (Table 5). These included fluoranthene (71% increase), benz(*j/k*)fluoranthene (6710% increase), benz(*a*)fluoranthene (not calculable increase owing to its absence in floating oils), benzo(*a*)pyrene (120% increase), indeno(1,2,3-*cd*)pyrene (368% increase) and benzo(*g,h,i*)perylene (57% increase). These increases owe largely to the low concentrations of these particular PAHs in both the fresh and naturally-weathered floating Macondo oils (Table 2), but nonetheless demonstrate some additional load of selected pyrogenic PAH was caused by *in-situ* burning. As stated above, however, *in-situ* burning of 258,800 to 364,700 bbl of oil markedly reduced the load of PAHs to surface water of the GoM (~89% total reduction; Table 5), although it increased the load of PAHs to the benthos (Table 4).

4. Conclusions

Between April 28 and July 19, 2010, 411 separate *in-situ* burn (ISB) events were conducted to reduce the quantity of oil floating on the sea in response to the *Deepwater Horizon* (DWH) oil spill. Despite the large volume of oil consumed by these countermeasure events, tens of thousands of barrels of ISB residues were generated. Our results, based upon decrease in chromatographable mass relative to hopane, suggest burn efficiencies were on the order of 85%. Calculated from the previously-reported range in the volume of oil consumed in the ISB events (220,000 to 310,000 barrels; bbls), we estimated that between 38,800 and 54,700 bbl of ISB residue were generated in the northern Gulf of Mexico and most or all of this eventually sank to the seafloor.

The specific chemical compositions of two floating ISB residues collected immediately following their respective burn events were studied using GC/FID and GC/MS and found to exhibit features distinct from naturally-weathered floating oils. Quantitative comparisons were made using hopane as a conservative internal marker compound. These distinct features were also exhibited by two discrete "lumps" of oil residues collected from the sediment surface using a remotely operated vehicle, which demonstrated at least some ISB residues indeed had sunk (~1,400 m) to the seafloor. The floating and sunken ISB residues of Macondo crude oil were chemically distinguishable from naturally-weathered (mostly evaporated) floating oil collected during the DWH spill.

Using hopane as a conservative internal marker, ISB residues were shown to contain higher concentrations of *n*-alkanes below *n*-C_{18} and lower concentrations of *n*-alkanes between *n*-C_{19} and *n*-C_{30}, and also exhibited similarly distinct UCM profiles. This indicates that the ISB residues experienced complex distillation/combustion processes – and not simply the vapor pressure-driven evaporation experienced by floating (unburned) oils. We hypothesize that the ISB residues had experienced preferential and more rapid combustion of some C_{19}+ *n*-alkanes and other homologous hydrocarbons within the UCM due to the decrease in ignition temperatures and increase in cetane number with increasing carbon number.

As observed in previous studies of ISB residues, the ISB residues studied herein were relatively enriched in combustion-derived (pyrogenic) PAHs (relative to hopane) compared to unburned floating oil. These pyrogenic PAHs were likely formed by intense heating within the oil and/or from soot particles that condensed within the fire's smoke that were re-deposited within the floating ISB residue before it sank. Isomer specific PAH enrichments were evident in the burn residues that were consistent with combustion. Specifically, anthracene, fluoranthene, benz(*a*)anthracene, benzo(*j/k*)fluoranthene and benzo(a)pyrene were formed preferentially over phenanthrene, pyrene, chrysene, benzo(*b*)fluorene, and benzo(*e*)pyrene, respectively. The preferential formation of less stable linear (or mostly linear) PAH isomers over others (e.g., anthracene over phenanthrene, fluoranthene over pyrene and benz(*a*)anthracene over chrysene) is consistent with the rapid, high temperature heating and the relatively rapid quenching reactions associated with combustion.

Although terpane and sterane biomarker distributions appear qualitatively comparable after *in-situ* burning, quantitative analysis shows some depletions among these normally resistant compounds occurred. Specifically, the percent depletions of tricyclic terpanes, dia- and regular steranes, and C_{27} to C_{35} hopanes increase with shorter relative retention times (i.e., greater volatility) indicating these compounds were variably volatilized during *in-situ* burning. Hopane itself appears to have evaporated relative to C_{31}+ homohopanes, which indicates that the percent depletions of *n*-alkanes, PAHs and other hydrocarbons (calculated relative to hopane) described above are likely underestimated. Notably, triaromatic steroids were also depleted due to evaporation during *in-situ* burning but also demonstrate an additional (~20%) depletion attributed to their photo-oxidation in the floating oils prior to *in-situ* burning.

PAH concentrations in the ISB residues were used to estimate between 26,800 and 37,800 kg of total PAHs (TPAH51) were potentially deposited on the seafloor within discrete ISB residue particles. Despite this additional impact to the benthos, the overall effect of *in-situ* burning must also consider the reduction in total mass loadings of PAH to the GoM surface water (and ultimately perhaps shorelines) if *in-situ* burning was not performed in response to the DWH oil spill. If the 258,800 to 364,700 bbl of floating Macondo oil subjected to *in-situ* burning had not been burned, a total of approximately 242,000 to 340,000 kg of total PAH (TPAH51) would have remained within surface slicks and/or the uppermost water column, perhaps ultimately reaching shorelines. Thus, *in-situ* burning reduced the total loading of PAHs from the burned oil to the Gulf of Mexico by 89% (ignoring any re-deposition of soot and aerosols from the emissions). When the mass loadings of individual PAHs are considered, *in-situ* burning reduced input of all but six pyrogenic, high molecular weight PAHs, the increases of which owe largely to their low concentrations in fresh Macondo oil.

Acknowledgements

The authors thank Dr. Scott Miles, Louisiana State University, who provided the floating *in-situ* burn samples studied and Mr. Alan Allen, Spiltec for discussing his first-hand experience with *in-situ* burning that occurred in response to the DWH oil spill. The authors also wish to acknowledge Wendy Wong and Eric Litman (NewFields) who managed the chemical analysis conducted by the Alpha Analytical Laboratory staff.

Disclosure

This study was conducted within the Deepwater Horizon NRDA investigation, which was cooperatively conducted by NOAA, other Federal and State Trustees, and BP. The scientific results and conclusion of this publication, as well as any views or opinions expressed herein, are those of the authors only. The authors declare no competing financial interest in the publication of this study. Funding for the study was provided by NOAA through Industrial Economics, Corp. (Cambridge, MA) as part of the NRDA process.

References

Aeppli, C., Nelson, R.K., Radović, J.R., Carmichael, C.A., Valentine, D.L., Reddy, C.M., 2014. Recalcitrance and degradation of petroleum biomarkers upon abiotic and biotic natural. weathering of Deepwater Horizon oil. *Environ. Sci. Technol.* 48: 6726-6734.

Allen, A.A., 2011. I*n*-situ burn operations during *Deepwater Horizon* oil spill. OSPR/Chevron Oil Spill Response Technical Workshop, San Ramon, CA Feb. 15-17, 2011. https://nrm.dfg.ca.gov/FileHandler.ashx?DocumentID=29439, accessed July 2014.

American Petroleum Institute, 2002, Identification of oils that produce non-buoyant in situ burning residues and methods for their recovery. API DR145, Report by S.L. Ross Environmental Research Ltd., American Petroleum Institute, Washington, D.C., 69 pp.

Budzinski, H., Jones, I., Bellocq, J., Pierard, C. Garrigues, P. 1997. Evaluation of sediment contamination by polycyclic aromatic hydrocarbons in the Gironde estuary. *Marine Chemistry* **58**: 85-97.

Buist, I., Trudel, K., Morrison, J., Aurand, D. 1997. Laboratory Studies of the Properties of In situ Burn Residues, Proc. Int'l. Oil Spill Conference, p. 149-156.

Dickhut, R. M., Canuel, E. A., Gustafson, K. E., Liu, K., Arzayus, K. M., Walker, S. E., Edgecombe, G., Gaylor, M. O., MacDonald, E. H. 2000. Automotive sources of carcinogenic polycyclic aromatic hydrocarbons associated with particulate matter in the Chesapeake Bay region. *Environmental Science and Technology* **34**(21): 4635-4640.

Douglas, G.S., Emsbo-Mattingly, S.D., Stout, S.A., Uhler, A.D., McCarthy, K.J. 2015. Hydrocarbon fingerprinting methods. In: Introduction to Environmental. Forensics, 3rd Ed., B.L. Murphy and R.D. Morrison, Eds., Academic Press, Boston, pp. 201-309.

Evans, D.D., Mullholland, G.W., Baum, H.R., Walton, W.D., McGrattan, K.B., 2001. In-situ burning of oil spills. *J. Res. Natl. Inst. Stand. Technol.* **106**(1): 231-278.

Fingas, M., 2011. "An Overview of In-situ Burning". *Oil Spill Science and Technology*. Boston, Elsevier**:** 737-903.

Garrett, R. M., Guénette, C. D., Haith, C. E., Prince, R. C. 2000. Pyrogenic polycyclic aromatic hydrocarbons in oil burn residues. *Environmental Science and Technology* **34**(10): 1934-1937.

Garrett, R. M., Pickering, I. J., Haith, C. E., Prince, R. C. 1998. Photooxidation of crude oils. *Environmental. Science and Technology* 32(23): 3719-3723.

Hites, R. A., Laflamme, R. E., Farrington, J. W. 1977. Sedimentary polycyclic aromatic hydrocarbons: the historical record. *Science* 198: 829-831.

Lee, R. F. 2003. Photooxidation and phototoxicity of crude and refined oils. *Spill Sci. Technol. Bull*. 8: 157-162.

Mabile, N., Allen, A. 2010. Controlled burns - After-action report. Controlled Burn Group Report, dated Aug. 8, 2010.

Merker, G.P., Schwarz, C., Teichmann, R. 2012. Combustion Engines Development: Mixture Formation, Combustion, Emissions, and Simulation. Springer-Verlag, Berlin, 642 p.

Moller, T.H., 1992, Recent experience of oil sinking. Proc. Fifteenth Arctic and Marine Oilspill, Program Technical Seminar, Environment Canada, Ottawa, Ontario, pp. 11-14.

NOAA ,1992. Oil Spill Case Histories 1967-1991. Summaries of significant U.S. and International Spills. NOAA Report No. HMRAD 92-11, Seattle, WA.

NOAA, 2014. Residues from in-situ burning on oil on water. Office of Response and Restoration. http://response.restoration.noaa.gov/oil-and-chemical-spills/oil-spills/resources/residues-in-situ-burning-oil-water.html, accessed April 2014.

Perring, A. E., Schwarz, J. P., Spackman, J.R., Bahreini, R., deGouw, J.A., Gao, R.S., Holloway, J.S., Lack, D.A., Langridge, J.M., Peischl, J., Middlebrook, A.M., Ryerson, T.B., Warneke, C., Watts, L.A., Fahey, D.W. 2011. Characteristics of black carbon aerosol from a surface oil burn during the Deepwater Horizon oil spill. *Geophys. Res. Letters* **38**(L17809): 5 pp.

Plata, D.L., Sharpless, C.M., Reddy, C.M., 2008. Photochemical degradation of polycyclic aromatic hydrocarbons in oil films. *Environ. Sci. Technol.* 42: 2432-2438.

Prince, R. C., Elmendorf, D. L., Lute, J. R., Hsu, C. S., Haith, C. E., Senius, J. D., Dechert, G. J., Douglas, G. S., Butler, E. L. 1994. 17a(*H*),21b(*H*)-hopane as a conserved internal marker for estimating the biodegradation of crude oil. *Environmental Science and Technology* **28**(1): 142-145.

Ryerson, T. B., Aikin, K.C., Angevine, W.M., Atlas, E.L., Blake, D.R., Brock, C.A., Fehsenfeld, F.C., Gao, R-S, deGouw, J.A., Fahey, D.W., Holloway, J.S., Lack, D.A., Lueb, R.A., Meinardi, S., Middlebrook, A.M., Murphy, D. M., Neuman, J.A., Nowak, J.B., Parrish, D.D., Peischl, J., Perring, A.E., Pollack, I.B., Ravishankara, A.R., Roberts, J. M., Schwarz, J. P., Spackman, J.R., Stark, H., Warneke, C., Watts, L.A. 2011. Atmospheric emissions from the Deepwater Horizon spill constrain air-water partitioning, hydrocarbon fate, and leak rate. *Geophys. Res. Letters* **38**(L07803): 6 pp.

Shigenaka, G., Overton, E., Meyer, B.M., Gao, H., Miles, S. 2015. Physical and chemical characteristics of i*n*-situ burn residue and other environmental oil samples collected during the Deepwater Horizon spill response. Proc. Interspill 2015, Amsterdam, March 24-26, 2015, 11 p.

Shimy, A.A., 1970. Calculating flammability characteristics of hydrocarbons and alcohols. *Fire Technol*. 6: 135-139.

Stauffer, E., Dolan, J. A., Newman, R. 2008. Fire Debris Analysis. Elsevier, Burlington, MA., 634 pp.

Stout, S.A., Payne, J.R., Emsbo-Mattingly, S.D., Baker, G. (2016). Weathering of Field-Collected Floating and Stranded Macondo Oils during and shortly after the Deepwater Horizon Oil Spill. Mar. Pollut. Bull, Available on-line Feb. 28, 2016.

Walavalkar, A.Y. 2001. Combustion of water-in-oil emulsions of diesel and fresh and weathered crude oils floating on water. Ph.D. Thesis, The Pennsylvania State University, Aug. 2001.

Wang, Z., Fingas, M., Shu, Y. Y., Sigouin, L., Landriault, M., Lambert, P., Turpin, R., Campagna, P., Mullin, J. 1999. Quantitative Characterization of PAHs in Burn Residue and Soot Samples and Differentiation of Pyrogenic PAHs from Petrogenic PAHs – The 1994 Mobile Burn Study. *Environmental Science and Technology* **33**(18): 3100-3109.

Wang, Z.. Stout, S.A., Fingas, M. (2006) Forensic fingerprinting of biomarkers for oil spill characterization and source identification (Review). *Environ. Forensics* 7(2): 105-146.

Yunker, M. B., Macdonald, R. W., Vingarzan, R., Mitchell, R. H., Goyette, D., Sylvestre, S. 2002. PAHs in the Fraser River basin: a critical appraisal of PAH ratios as indicators of PAH source and composition. *Organic Geochemistry* **33**: 489-515.

Table 1: Burn residue sample descriptions.

Sample ID	Abbrev.	Lab ID	Date Collected	Latitude	Longitude	Water Depth (m)	Description
Floating Burn Residues							
5-05-2010 Burn Residue from Burn #2	#2	1203046-01	May 5, 2010	28 38.99 N	-88 21.735 W	0	tarry residue from Burn #2, collected by N. Mabile. 512 to 716 bbl consumed.
5-19-2010 Burn #4 Residue	#30	1203046-02	May 19, 2010	28 52.84 N	-88 17.68 W	0	tarry residue from Burn #30 (4th burn on May 19), 769 to 1076 bbl consumed.
Sunken Burn Residues							
HSW6_FP10187A_B0827_O_1429_50_0082	#82	1201017-01	Aug. 27, 2011	28.45.63 N	-88 22.37 W	1429	tar-like semi-solid (~ 3 cm diam.), collected J. Payne (ROV)
HSW6_FP10187B_B0827_O_1434_50_0083	#83	1201017-02	Aug. 27, 2011	28.45.78 N	-88 22.05 W	1434	tar-like fluid (smeared within core barrel), collected by J. Payne (ROV)
HSW6_FP10187C_B0827_F_1433_50_PB_0076	#76	1108075-06	Aug. 27, 2011	28.45.81 N	-88 22.00 W	1433	tar-like semi-solid (~ 1 cm diam.), collected by J. Payne (ROV)

Table 2: Concentrations ($\mu g/g_{oil}$) of PAH analytes and hopane and various totals in fresh Macondo oil, floating (unburned) Macondo crude oils, and in the floating and sunken burn residues studied herein. Concentrations are non-surrogate corrected. Priority Pollutant PAHs (16) indicated by italics. Bold values for burn residues exceed all concentrations for fresh and floating oils.

Abbrev	Analytes	Fresh Macondo Oil (Avg; n=6)	Floating (Unburned) Oils			Floating ISB Residue		Sunken ISB Residue		
			Average (n=62)	Minimally Weathered[a]	Severely Weathered[b]	#2	#30	#82	#83	#76 [c]
N0	*Naphthalene*	964	31	346	0.18	2.3	4.1	1.7	4.4	408
N1	C1-Naphthalenes	2106	234	1607	0.53	13	20	4.0	38	1132
N2	C2-Naphthalenes	2259	587	2371	1.3	76	108	24	231	1864
N3	C3-Naphthalenes	1597	609	1646	3.1	112	184	57	428	1310
N4	C4-Naphthalenes	721	363	752	7.5	84	142	59	369	**1310**
B	Biphenyl	204	41	197	0.23	2.4	3.8	0.31	10	6.3
DF	Dibenzofuran	30	11	35	0.18	1.5	2.4	0.69	3.9	**54**
AY	*Acenaphthylene*	8.9	3.0	9.4	0.06	4.1	4.7	8.6	**21**	**32**
AE	*Acenaphthene*	21	8.1	28	0.08	1.4	1.8	0.75	5.9	**64**
F0	*Fluorene*	150	60	180	0.76	10	19	6.8	38	56
F1	C1-Fluorenes	308	185	391	5.3	41	74	30	137	33
F2	C2-Fluorenes	404	293	485	22	86	144	86	319	297
F3	C3-Fluorenes	286	247	334	40	99	152	101	309	**1311**
A0	*Anthracene*	2.3	3.9	nd	nd	2.8	**4.4**	**7.3**	**37**	**1499**
P0	*Phenanthrene*	310	201	411	14	59	105	54	193	**1025**
PA1	C1-Phenanthrenes/Anthracenes	676	569	862	101	197	309	184	513	110
PA2	C2-Phenanthrenes/Anthracenes	657	650	805	180	263	372	292	698	18
PA3	C3-Phenanthrenes/Anthracenes	381	355	412	98	180	245	192	**435**	19
PA4	C4-Phenanthrenes/Anthracenes	148	150	176	40	84	113	84	**193**	39
DBT0	Dibenzothiophene	53	33	69	1.5	8.2	15	6.4	23	**379**
DBT1	C1-Dibenzothiophenes	153	128	202	16	44	67	27	84	**655**
DBT2	C2-Dibenzothiophenes	197	199	245	51	82	117	79	187	**505**
DBT3	C3-Dibenzothiophenes	146	162	178	53	77	105	78	163	30
DBT4	C4-Dibenzothiophenes	72	80	86	29	41	64	41	79	**314**
BF	Benzo(b)fluorene	11	7.5	17	nd	6.0	8.1	nd	**31**	**730**
FL0	*Fluoranthene*	4.1	3.6	5.8	0.66	**8.0**	**11**	**20**	**100**	**762**
PY0	*Pyrene*	16	15	21	2.0	18	**24**	**37**	**187**	**437**
FP1	C1-Fluoranthenes/Pyrenes	80	76	106	13	51	71	nd	**194**	**181**
FP2	C2-Fluoranthenes/Pyrenes	130	124	177	17	89	123	114	**213**	nd
FP3	C3-Fluoranthenes/Pyrenes	158	154	208	33	119	166	149	**255**	34
FP4	C4-Fluoranthenes/Pyrenes	125	139	177	43	112	146	127	**200**	132
NBT0	Naphthobenzothiophenes	18	27	29	13.6	17	22	21	**38**	**187**
NBT1	C1-Naphthobenzothiophenes	56	79	91	38.8	50	68	60	**93**	**152**
NBT2	C2-Naphthobenzothiophenes	80	100	114	39	77	100	84	**126**	84
NBT3	C3-Naphthobenzothiophenes	58	70	90	19.0	59	75	63	**90**	12
NBT4	C4-Naphthobenzothiophenes	37	48	64	11.3	37	49	42	64	41
BA0	*Benz[a]anthracene*	7.3	5.0	7.6	nd	**7.7**	**10**	**15**	**59**	**114**
C0	*Chrysene/Triphenylene*	56	68	64.1	40.1	47	60	64	**125**	**185**
BC1	C1-Chrysenes	129	139	160	59	111	145	127	**204**	**194**
BC2	C2-Chrysenes	158	153	194	43	137	180	148	**268**	150
BC3	C3-Chrysenes	156	129	192	23	143	183	150	**263**	106
BC4	C4-Chrysenes	90	77	113	15	88	111	90	**155**	21
BBF	*Benzo[b]fluoranthene*	6.1	7	6.8	4.4	**8.8**	**11**	**16**	**46**	**50**
BJKF	*Benzo[jk]fluoranthene*	0.5	0.04	nd	nd	**3.7**	**3.8**	**11**	**36**	**65**
BAF	Benzo[a]fluoranthene	0.7	nd	nd	nd	**2.6**	**3.0**	**5.8**	**18**	**44**
BEP	Benzo[e]pyrene	12	14	15	5.3	**15**	**18**	**26**	**57**	**35**
BAP	*Benzo[a]pyrene*	3.2	2.4	3.8	nd	**7.8**	**8.9**	**20**	**84**	**14**
PER	Perylene	1.0	0.78	1.4	nd	1.9	2.4	2.4	**12**	**51**
IND	*Indeno[1,2,3-cd]pyrene*	1.2	0.59	1.2	nd	**4.2**	**4.6**	**11**	**43**	**98**
DA	*Dibenz[a,h]anthracene*	2.5	1.9	2.6	nd	**3.2**	**3.6**	**5.7**	**11**	**122**
GHI	*Benzo[g,h,i]perylene*	2.3	2.4	2.6	0.72	**6.7**	**7.7**	**16**	**57**	**113**
T19	Hopane	69	112	81	144	84	104	117	**149**	61
Total Concentrations (µg/g oil)										
TEM (C9-C44)		681,000	601,144	736,920	518,000	274,000	380,000	311,000	624,000	682,000
TPAH51 (ΣN0-GHI)		13,252	6643	13,685	1087	2797	3990	2850	7549	**16,585**
HPAH (ΣBF-GHI)		1399	1443	1861	421	1228	1615	1424	**3030**	**4116**
Priority Pollutant TPAH16		1555	412	1089	0	194	284	294	1049	**5046**

[a] JF3-2km-onet-20100616-surf-N143

[b] GU-10-02-005-T-003

[c] all conc. affected by distillate component

Table 3: Concentrations ($\mu g/g_{oil}$) of biomarker analytes in fresh Macondo oil and in the floating and sunken burn residues studied herein. Concentrations are non-surrogate corrected.

		Fresh Macondo Oil (Avg; n=6)	Floating ISB Residue		Sunken ISB Residue		
Abbrev	Biomarker Analyte		#2	#30	#82	#83	#76 *
T4	C23 Tricyclic Terpane	10	6	9	5	11	20
T5	C24 Tricyclic Terpane	7	5	7	5	7	11
T6	C25 Tricyclic Terpane	10	9	10	7	15	9
T6a	C24 Tetracyclic Terpane	3	3	4	5	6	3
T6b	C26 Tricyclic Terpane-22S	7	6	7	7	10	6
T6c	C26 Tricyclic Terpane-22R	5	4	3	4	7	4
T7	C28 Tricyclic Terpane-22S	3	3	4	5	6	3
T8	C28 Tricyclic Terpane-22R	4	4	5	5	6	3
T9	C29 Tricyclic Terpane-22S	5	5	6	5	9	4
T10	C29 Tricyclic Terpane-22R	4	5	6	4	8	3
T11	18α-22,29,30-Trisnorneohopane-Ts	14	14	18	17	23	11
T11a	C30 Tricyclic Terpane-22S	4	5	7	6	8	3
T11b	C30 Tricyclic Terpane-22R	4	6	6	8	9	5
T12	17α(H)-22,29,30-Trisnorhopane-Tm	11	12	15	14	19	9
T14a	17α/β,21β/α 28,30-Bisnorhopane	5	7	8	10	14	5
T14b	17α(H),21β(H)-25-Norhopane	2	4	4	4	6	2
T15	30-Norhopane	29	35	43	47	71	27
T16	18α(H)-30-Norneohopane-C29Ts	11	14	17	17	25	9
X	17α(H)-Diahopane	9	10	13	11	15	7
T17	30-Normoretane	4	7	7	8	11	5
T18	18α(H)&18β(H)-Oleananes	3	4	4	3	5	3
T19	Hopane	69	84	104	117	149	61
T20	Moretane	9	10	12	14	14	9
T21	30-Homohopane-22S	29	38	45	45	64	26
T22	30-Homohopane-22R	24	31	40	38	60	21
T26	30,31-Bishomohopane-22S	20	26	30	35	49	18
T27	30,31-Bishomohopane-22R	15	20	25	26	37	13
T30	30,31-Trishomohopane-22S	16	22	27	29	44	14
T31	30,31-Trishomohopane-22R	11	16	20	19	29	11
T32	Tetrakishomohopane-22S	11	15	19	19	28	11
T33	Tetrakishomohopane-22R	8	12	12	15	20	7
T34	Pentakishomohopane-22S	8	12	14	17	26	8
T35	Pentakishomohopane-22R	7	10	11	14	26	6
S4	13β(H),17α(H)-20S-Diacholestane	54	49	60	48	80	38
S5	13β(H),17α(H)-20R-Diacholestane	31	29	35	30	47	23
S8	13β,17α-20S-Methyldiacholestane	23	24	31	26	45	19
S12/S13	14α(H),17α(H)-20S-Cholestane + 13β(H),17α(H)-20S-Ethyldiacholestane	62	63	79	76	104	49
S17/S18	14α(H),17α(H)-20R-Cholestane + 13β(H),17α(H)-20R-Ethyldiacholestane	72	72	79	78	115	54
S18x	Unknown sterane	15	19	22	18	27	12
S19	13α,17β-20S-Ethyldiacholestane	2	3	4	3	4	2
S20	14α,17α-20S-Methylcholestane	30	30	37	27	46	21
S24	14α,17α-20R-Methylcholestane	25	27	31	32	44	18
S25	14α(H),17α(H)-20S-Ethylcholestane	38	39	47	49	67	31
S28	14α(H),17α(H)-20R-Ethylcholestane	26	31	36	39	55	21
S14	14β(H),17β(H)-20R-Cholestane	33	31	39	39	54	25
S15	14β(H),17β(H)-20S-Cholestane	31	31	41	37	53	25
S22	14β(H),17β(H)-20R-Methylcholestane	32	33	39	39	56	25
S23	14β(H),17β(H)-20S-Methylcholestane	37	39	51	48	70	33
S26	14β(H),17β(H)-20R-Ethylcholestane	44	46	50	58	84	38
S27	14β(H),17β(H)-20S-Ethylcholestane	30	30	40	31	39	20
RC26/SC27TA	C26,20R- +C27,20S- triaromatic steroid	144	131	165	130	201	92
SC28TA	C28,20S-triaromatic steroid	111	106	130	105	146	71
RC27TA	C27,20R-triaromatic steroid	87	82	104	81	119	56
RC28TA	C28,20R-triaromatic steroid	87	82	104	78	122	55

Table 4: Estimated mass loadings of PAHs to the seafloor due to sunken *in-situ* burn residues following DWH oil spill. Calculated from concentration data given in Table 2. Average mass loadings represent the average of all four ISB residues given the minimum and maximum estimated barrels (bbl) of residue formed from the 411 *in-situ* burn events during the DWH oil spill. Priority Pollutant PAHs (16) indicated by italics.

	Mass Loading of ISB Residue to Seafloor (g/bbl)					Average Mass Loading to Seafloor (kg)	
	Burn Residue #2	Burn Residue #30	Burn Residue #82	Burn Residue #83	Average (n=4)	38,800 bbl ISB Residue (min)	54,700 bbl ISB Residue (max)
Density (g/ml at 30°C; assumed)	0.95	0.95	1.05	1.05			
Naphthalene	0.34	0.62	0.29	0.74	0.50	19	27
C1-Naphthalenes	1.9	3.0	0.67	6.4	3.0	116	163
C2-Naphthalenes	11	16	4.1	39	18	682	962
C3-Naphthalenes	17	28	9.5	71	31	1218	1718
C4-Naphthalenes	13	21	10	62	26	1023	1442
Biphenyl	0.36	0.58	0.05	1.6	0.6	25	35
Dibenzofuran	0.23	0.36	0.12	0.7	0.3	13	19
Acenaphthylene	0.6	0.7	1.4	3.6	1.6	61	86
Acenaphthene	0.21	0.27	0.12	1.0	0.4	15	22
Fluorene	1.6	2.9	1.1	6.4	3.0	117	165
C1-Fluorenes	6.3	11	5.0	23	11	438	618
C2-Fluorenes	13	22	14	53	26	991	1397
C3-Fluorenes	15	23	17	52	27	1033	1456
Anthracene	0.42	0.66	1.2	6.2	2.1	83	117
Phenanthrene	8.8	16	9.0	32	16	639	901
C1-Phenanthrenes/Anthracenes	30	47	31	86	48	1871	2638
C2-Phenanthrenes/Anthracenes	40	56	49	117	65	2533	3571
C3-Phenanthrenes/Anthracenes	27	37	32	73	42	1639	2310
C4-Phenanthrenes/Anthracenes	13	17	14	32	19	736	1038
Dibenzothiophene	1.2	2.2	1.1	3.8	2.1	81	114
C1-Dibenzothiophenes	7	10	5	14	9	343	483
C2-Dibenzothiophenes	12	18	13	31	19	722	1018
C3-Dibenzothiophenes	12	16	13	27	17	656	924
C4-Dibenzothiophenes	6	10	7	13	9.0	349	492
Benzo(b)fluorene	0.91	1.2	0	5.2	1.8	71	100
Fluoranthene	1.2	1.6	3.4	17	6	222	314
Pyrene	2.7	3.6	6.1	31	11	424	598
C1-Fluoranthenes/Pyrenes	7.6	11	0	32	13	492	693
C2-Fluoranthenes/Pyrenes	13	19	19	36	22	840	1184
C3-Fluoranthenes/Pyrenes	18	25	25	43	28	1072	1511
C4-Fluoranthenes/Pyrenes	17	22	21	33	23	908	1280
Naphthobenzothiophenes	2.5	3.3	3.4	6.3	3.9	151	213
C1-Naphthobenzothiophenes	8	10	10	15	11	420	592
C2-Naphthobenzothiophenes	12	15	14	21	15	601	847
C3-Naphthobenzothiophenes	9	11	11	15	11	445	627
C4-Naphthobenzothiophenes	5.5	7.4	7.0	11	7.6	297	418
Benz[a]anthracene	1.2	1.6	2.5	10	3.8	146	206
Chrysene/Triphenylene	7.0	9.1	11	21	12	462	651
C1-Chrysenes	17	22	21	34	23	909	1282
C2-Chrysenes	21	27	25	45	29	1138	1604
C3-Chrysenes	22	28	25	44	30	1147	1617
C4-Chrysenes	13	17	15	26	18	686	967
Benzo[b]fluoranthene	1.3	1.7	2.6	7.7	3.3	129	183
Benzo[jk]fluoranthene	0.57	0.58	1.8	6.1	2.3	88	124
Benzo[a]fluoranthene	0.39	0.45	1.0	3.0	1.2	46	65
Benzo[e]pyrene	2.2	2.8	4.4	10	4.7	184	259
Benzo[a]pyrene	1.2	1.3	3.3	14	5.0	193	272
Perylene	0.29	0.36	0.41	2.1	0.8	30	43
Indeno[1,2,3-cd]pyrene	0.64	0.70	1.9	7.1	2.6	100	141
Dibenz[a,h]anthracene	0.49	0.54	1.0	1.8	0.9	37	52
Benzo[g,h,i]perylene	1.0	1.2	2.6	10	3.6	139	196
TPAH51 (ΣN0-GHI)	423	603	476	1260	690	26,800	37,800
HPAH (ΣBF-GHI)	184	243	238	501	291	11,300	15,900
Priority Pollutant TPAH16	29	43	49	175	74	2880	4060

Table 5: Comparison of mass loading (kg) of PAHs for unburned floating Macondo oil (average) and *in-situ* burn residues (average) and the percent mass reduction of PAH caused by the *in-situ* burning. On average, *in-situ* burning generally resulted in total mass reductions in excess of 80% for most PAHs (far right columns), whereas the total loadings of only a few high molecular weight PAHs were increased due to burning (bolded values). Priority Pollutant PAHs (16) indicated by italics.

	Mass of PAH in Unburned Naturally Weathered Floating Oil (Avg)			Mass of PAH Remaining in ISB Residue (from Table 4)			Percent Mass Reduction of PAH upon Burning the Oil	
	Avg (g/bbl)	kg (min bbl)[a]	kg (max bbl)[a]	Avg. (g/bbl)	kg (min bbl)	kg (max bbl)	(min bbl)	(max bbl)
Barrells [b]		258,800	364,700		38,800	54,700		
Naphthalene	4.3	1113	1569	0.50	19	27	98	98
C1-Naphthalenes	32.9	8511	11994	3.0	116	163	99	99
C2-Naphthalenes	82.4	21314	30036	18	682	962	97	97
C3-Naphthalenes	85.5	22133	31190	31	1218	1718	94	94
C4-Naphthalenes	50.9	13178	18570	26	1023	1442	92	92
Biphenyl	5.8	1489	2098	0.6	25	35	98	98
Dibenzofuran	1.6	412	580	0.3	13	19	97	97
Acenaphthylene	0.4	109	154	1.6	61	86	44	44
Acenaphthene	1.1	295	415	0.4	15	22	95	95
Fluorene	8.4	2168	3055	3.0	117	165	95	95
C1-Fluorenes	25.9	6702	9445	11	438	618	93	93
C2-Fluorenes	41.1	10632	14983	26	991	1397	91	91
C3-Fluorenes	34.6	8956	12620	27	1033	1456	88	88
Anthracene	0.5	140	198	2.1	83	117	41	41
Phenanthrene	28.3	7315	10308	16	639	901	91	91
C1-Phenanthrenes/Anthracenes	79.8	20652	29102	48	1871	2638	91	91
C2-Phenanthrenes/Anthracenes	91.2	23596	33252	65	2533	3571	89	89
C3-Phenanthrenes/Anthracenes	49.8	12880	18150	42	1639	2310	87	87
C4-Phenanthrenes/Anthracenes	21.0	5444	7671	19	736	1038	86	86
Dibenzothiophene	4.6	1196	1685	2.1	81	114	93	93
C1-Dibenzothiophenes	17.9	4636	6533	9	343	483	93	93
C2-Dibenzothiophenes	27.9	7214	10165	19	722	1018	90	90
C3-Dibenzothiophenes	22.7	5866	8266	17	656	924	89	89
C4-Dibenzothiophenes	11.3	2913	4105	9.0	349	492	88	88
Benzo(b)fluorene	1.1	272	384	1.8	71	100	74	74
Fluoranthene	0.50	130	183	6	222	314	**-71**	**-71**
Pyrene	2.0	528	744	11	424	598	20	20
C1-Fluoranthenes/Pyrenes	10.7	2771	3904	13	492	693	82	82
C2-Fluoranthenes/Pyrenes	17.4	4499	6339	22	840	1184	81	81
C3-Fluoranthenes/Pyrenes	21.6	5583	7868	28	1072	1511	81	81
C4-Fluoranthenes/Pyrenes	19.4	5030	7089	23	908	1280	82	82
Naphthobenzothiophenes	3.7	967	1362	3.9	151	213	84	84
C1-Naphthobenzothiophenes	11.1	2882	4062	11	420	592	85	85
C2-Naphthobenzothiophenes	14.1	3640	5130	15	601	847	83	83
C3-Naphthobenzothiophenes	9.9	2557	3603	11	445	627	83	83
C4-Naphthobenzothiophenes	6.7	1745	2459	7.6	297	418	83	83
Benz[a]anthracene	0.70	180	254	3.8	146	206	19	19
Chrysene/Triphenylene	9.5	2452	3455	12	462	651	81	81
C1-Chrysenes	19.5	5034	7094	23	909	1282	82	82
C2-Chrysenes	21.5	5572	7852	29	1138	1604	80	80
C3-Chrysenes	18.1	4683	6600	30	1147	1617	76	75
C4-Chrysenes	10.9	2811	3961	18	686	967	76	76
Benzo[b]fluoranthene	1.0	270	380	3.3	129	183	52	52
Benzo[jk]fluoranthene	0.005	1.3	1.8	2.3	88	124	**-6708**	**-6711**
Benzo[a]fluoranthene	nd	0	0	1.2	46	65	**nc**	**nc**
Benzo[e]pyrene	2.0	511	720	4.7	184	259	64	64
Benzo[a]pyrene	0.34	87	123	5.0	193	272	**-121**	**-121**
Perylene	0.11	28	40	0.8	30	43	**-7**	**-7**
Indeno[1,2,3-cd]pyrene	0.08	21	30	2.6	100	141	**-368**	**-368**
Dibenz[a,h]anthracene	0.26	68	95	0.9	37	52	46	46
Benzo[g,h,i]perylene	0.34	88	124	3.6	139	196	**-57**	**-58**
TPAH51 (ΣN0-GHI)	932	242,000	340,000	690	26,800	37,800	89	89
HPAH (ΣBF-GHI)	203	52,500	74,900	291	11,300	15,900	78	78
Priority Pollutant TPAH16	58	15,000	21,100	74	2880	4060	81	81

[a] density 0.8827 g/ml for weathered surface oil

[b] unburned oil total = consumed (220,000 to 310,000) + residue (38,800 to 54,700); ISB = residue only

nc - not calculable but large negative number

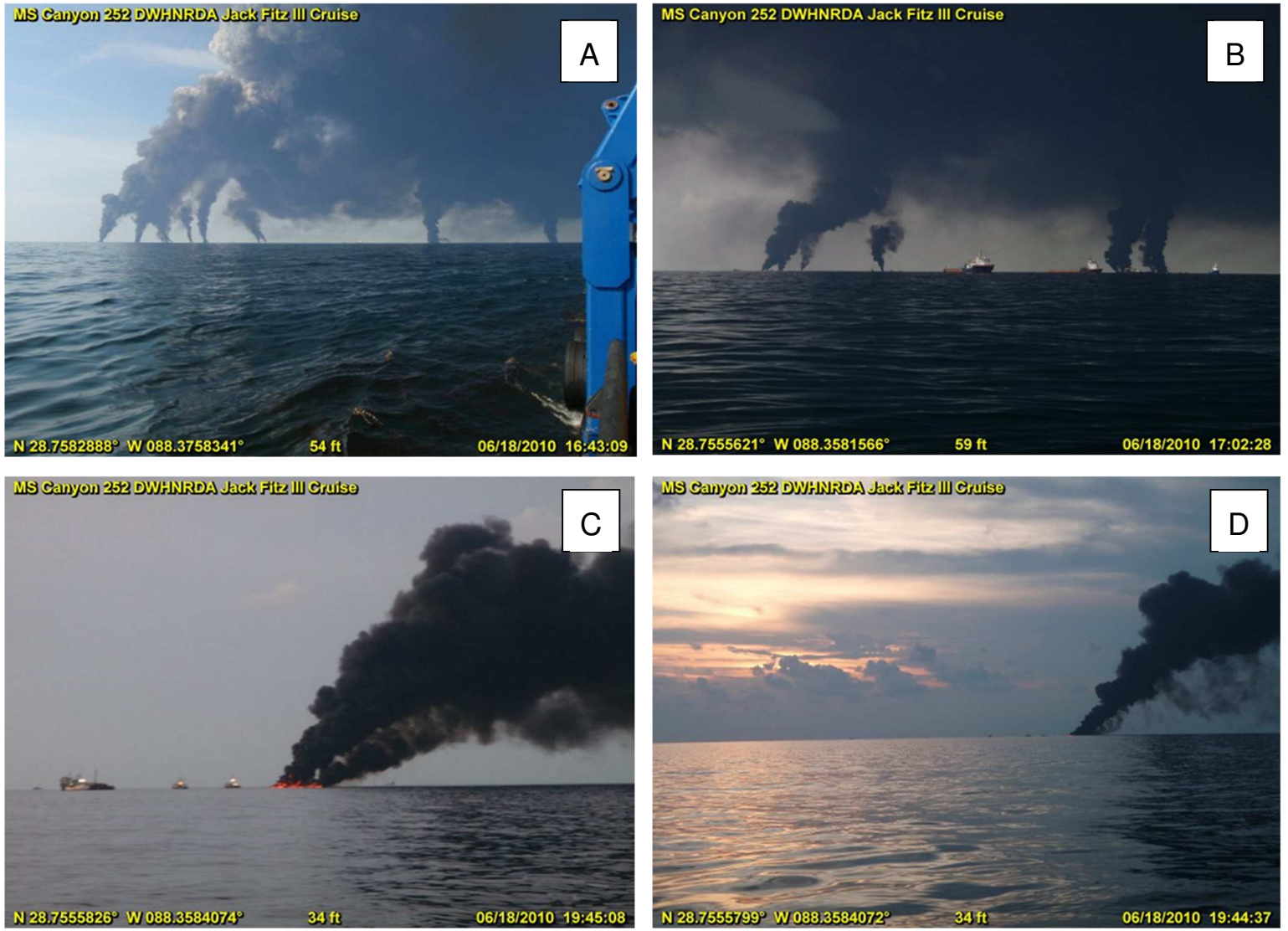

Figure 1. ***In-situ*** **burning operations on 18 June 2010 when 16 separate burn events occurred showing:** (A) proximity and extent of simultaneous burns; (B) intensity of smoke/soot generation; (C) localized nature of burning oil contained within fire boom; and (D) back-lit soot settling out of the plume and returning to the sea surface. Photographs by J.R. Payne.

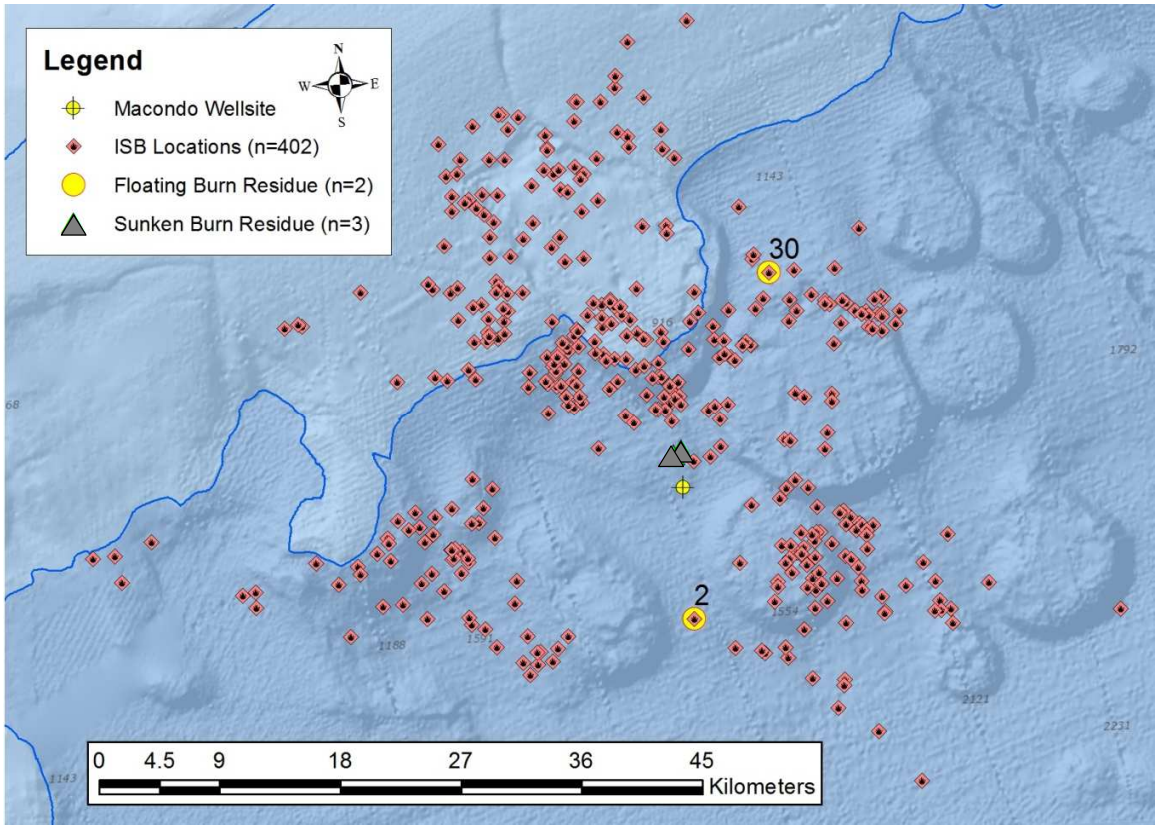

Figure 2: Map showing the locations for most of the 411 *in-situ* burns conducted between May 7 and July 19, 2010 and the locations of floating and sunken burn residue samples studied herein. 200 m bathymetric contour is shown. ISB locations obtained from Environmental Response Management Application (ERMA); http://response.restoration.noaa.gov/maps-and-spatial-data/environmental-response-management-application-erma; Locations of nine ISB events are unavailable.

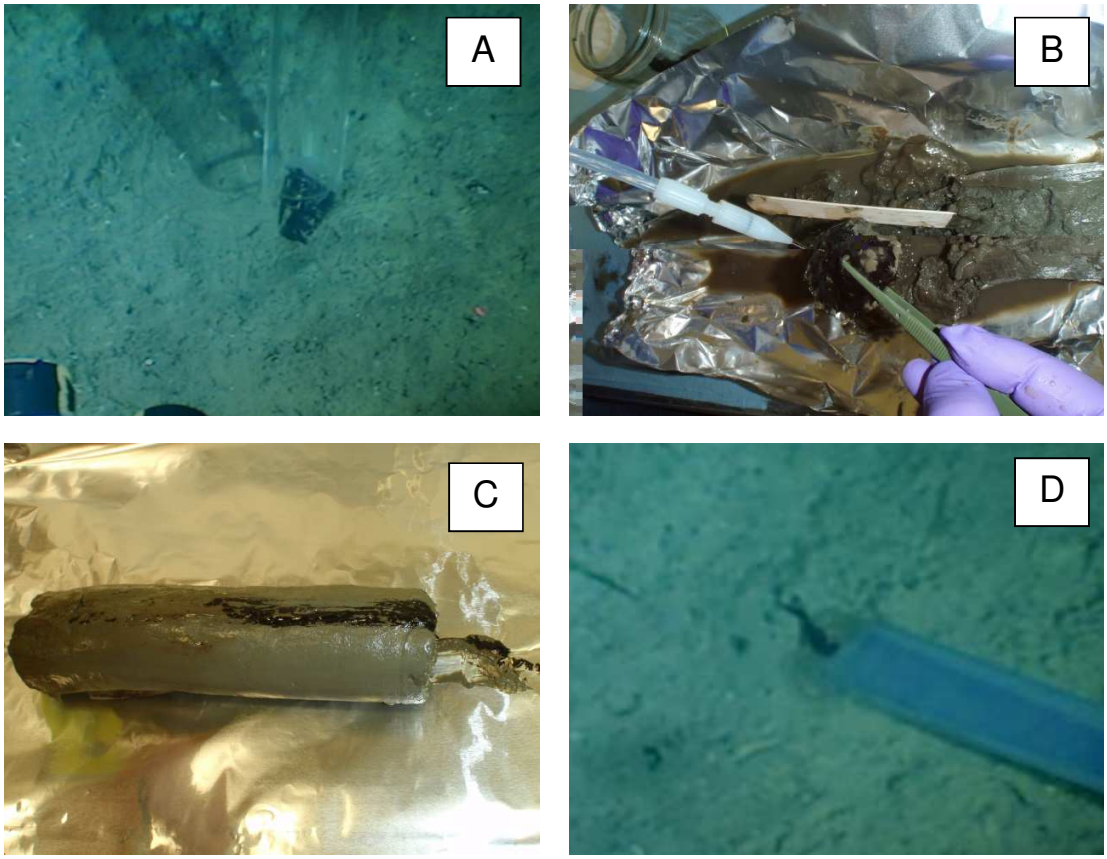

Figure 3: Photographs of the sunken burn residue samples studied herein. (A) core barrel collecting #82 sample from seafloor, (B) #82 tar-like semi-solid removed from extruded core, (C) #83 tar-like fluid that smeared along the core barrel on side of extruded core, and (D) #76 tarry flake sample being collected from seafloor with an ROV-mounted slurp-gun vacuum system. (Photographs by J.R. Payne).

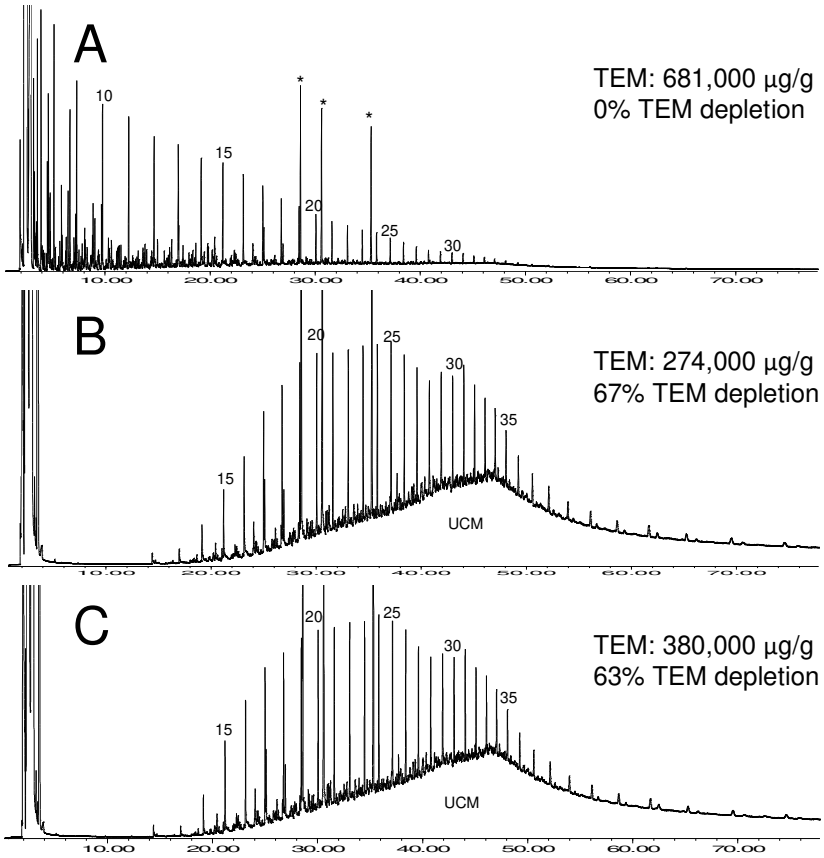

Figure 4: GC/FID chromatograms for (A) fresh Macondo oil (GU2988-A0521-O9805; 1005074-08), (B) floating ISB residue (Burn #2), and (C) floating ISB residue (Burn #30). * - internal standard; #: *n*-alkane carbon number, UCM: unresolved complex mixture. The concentrations of total extractable materials (TEM; C_9-C_{44}) are given along with the percent depletion in TEM relative to fresh Macondo oil (per Eq. 1). Data from Table 2.

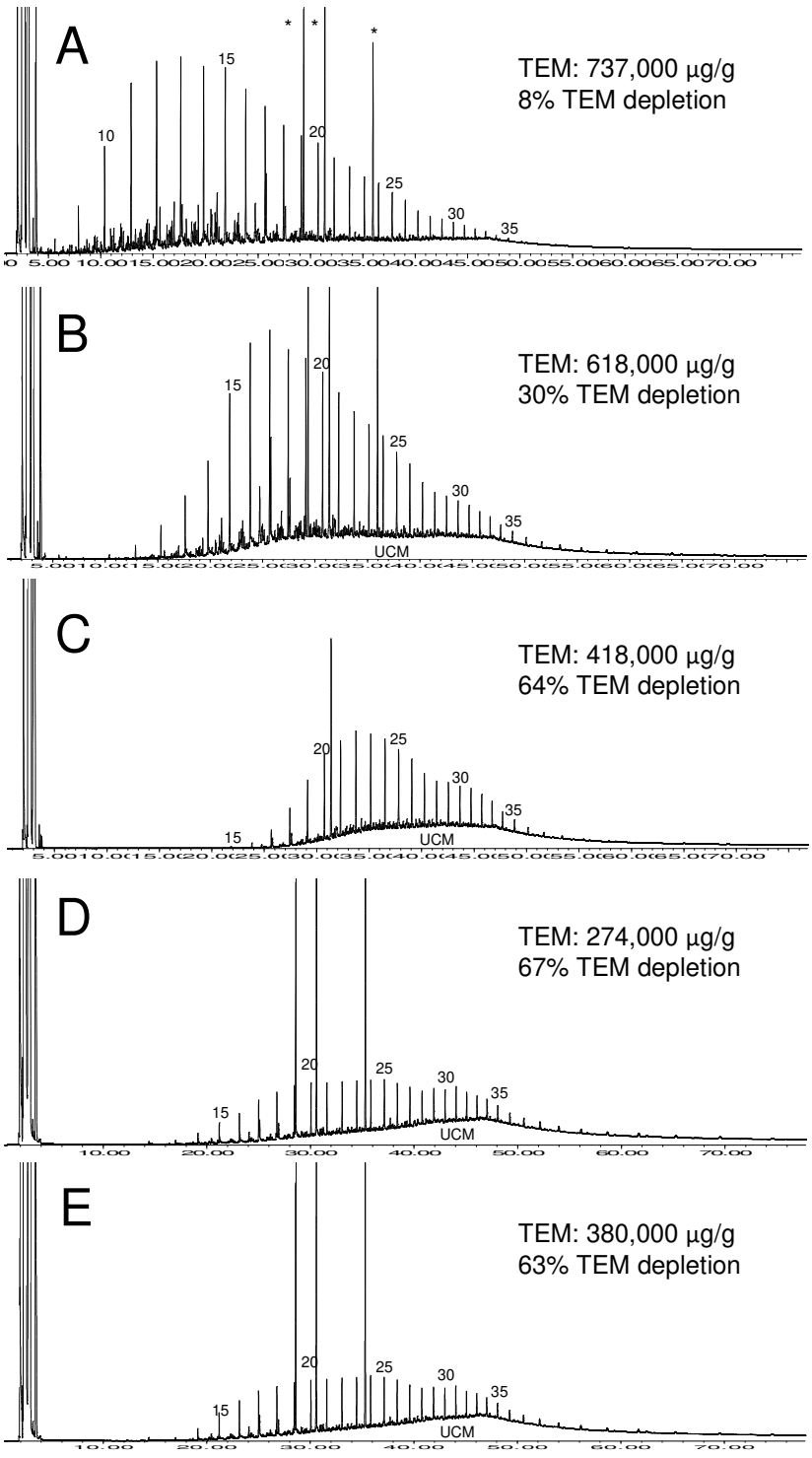

Figure 5: GC/FID chromatograms for (A) minimally evaporated floating oil (JF3-2km-onet-20100616-surf-N143), (B) moderately evaporated floating oil (JF2-4km-surf-0-20100524-N100) and (C) severely evaporated floating oil (GU-10-02005-T-003) compared to (D) floating ISB residue #2 and (E) floating ISB residue #30. The concentrations of total extractable materials (TEM; C_9-C_{44}) are given along with the percent depletion in TEM relative to fresh Macondo oil (per Eq. 1). * - internal standard; #: *n*-alkane carbon number; UCM – unresolved complex mixture.

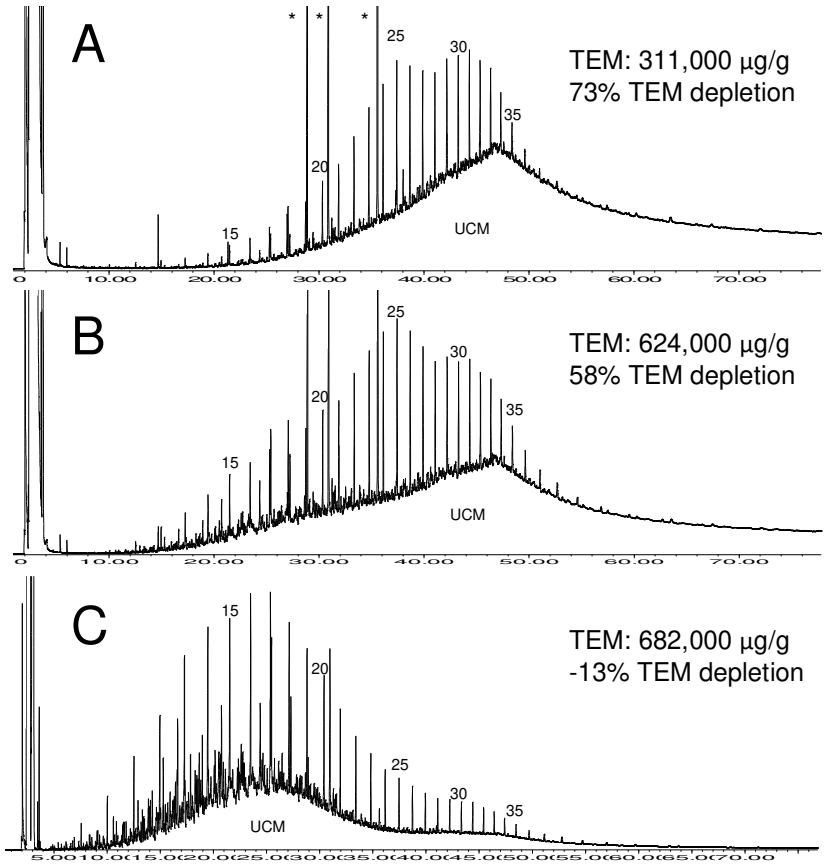

Figure 6: GC/FID chromatograms for sunken burn residues. (A) sunken ISB residue (#82), (B) sunken ISB residue (#83) and (C) unusual, tarry "flake" burn residue (#76 – see Fig. 3D). * - internal standard; #: *n*-alkane carbon number; UCM – unresolved complex mixture.

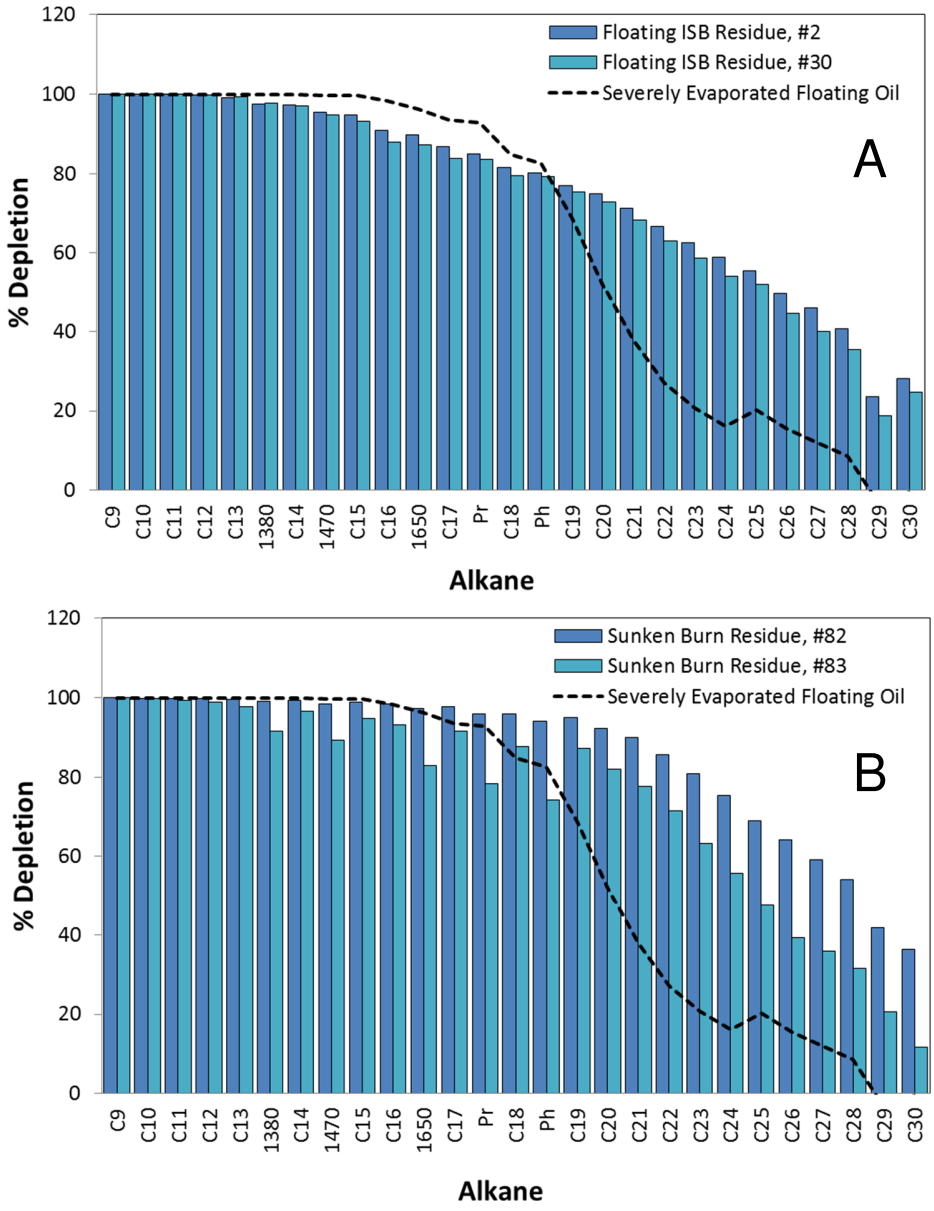

Figure 7: Percent depletion of *n*-alkanes and selected acyclic isoprenoids relative to hopane for (A) the floating burn residues and (B) sunken burn residues compared to severely evaporated (unburned) floating Macondo oil. The depletion of alkanes in the ISB residues is inconsistent with those typical of evaporation indicating ISB is not simply an evaporative process. Combustion and concomitant removal of long-chain alkanes is evident.

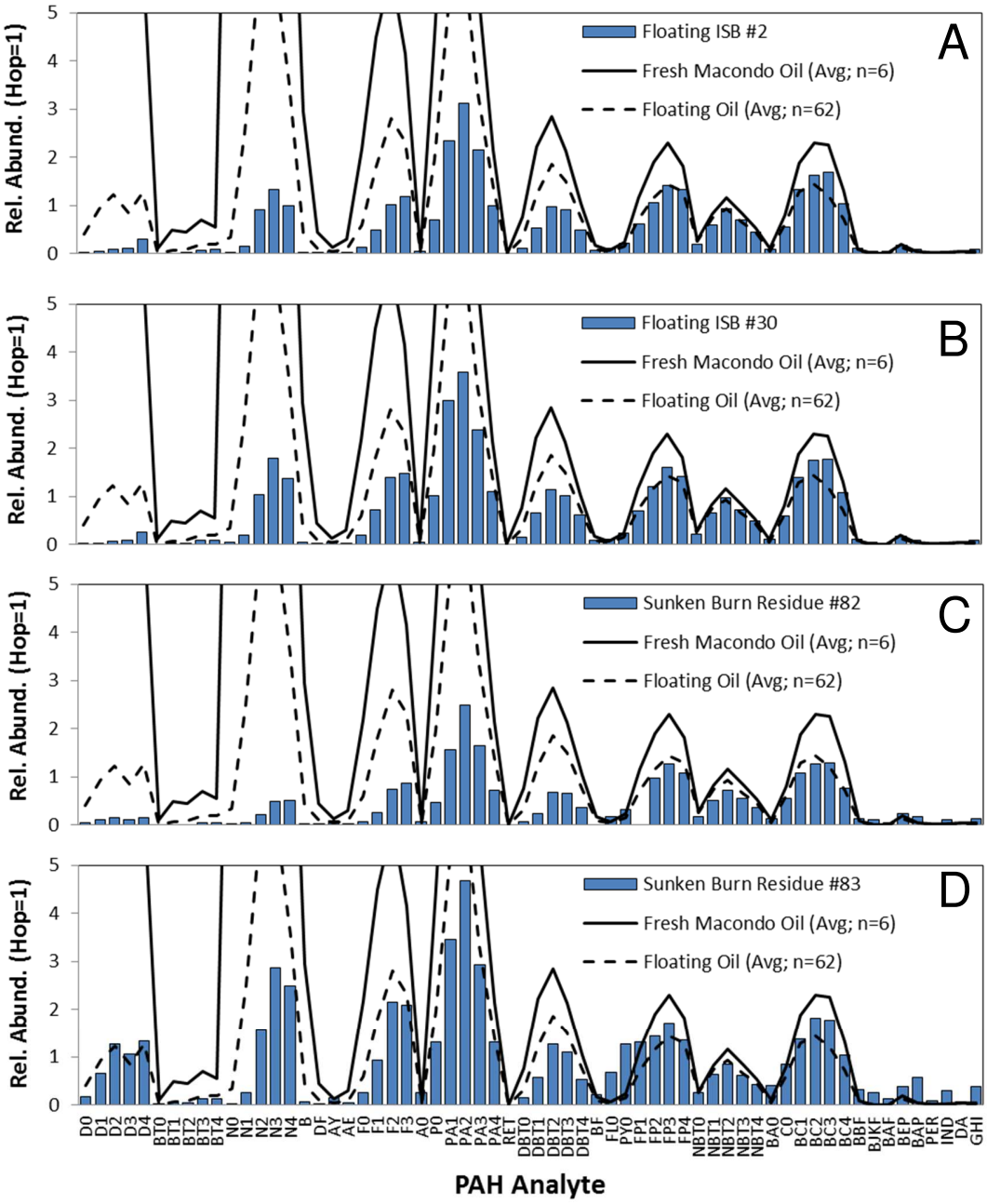

Figure 8: Hopane-normalized PAH histograms for the burn residues studied versus fresh and naturally-weathered (unburned) floating oil. (A) floating ISB residue #2, (B) floating ISB residue #30, (C) sunken ISB residue #82, and (D) sunken ISB residue #83. PAH analyte abbreviations from Table 2.

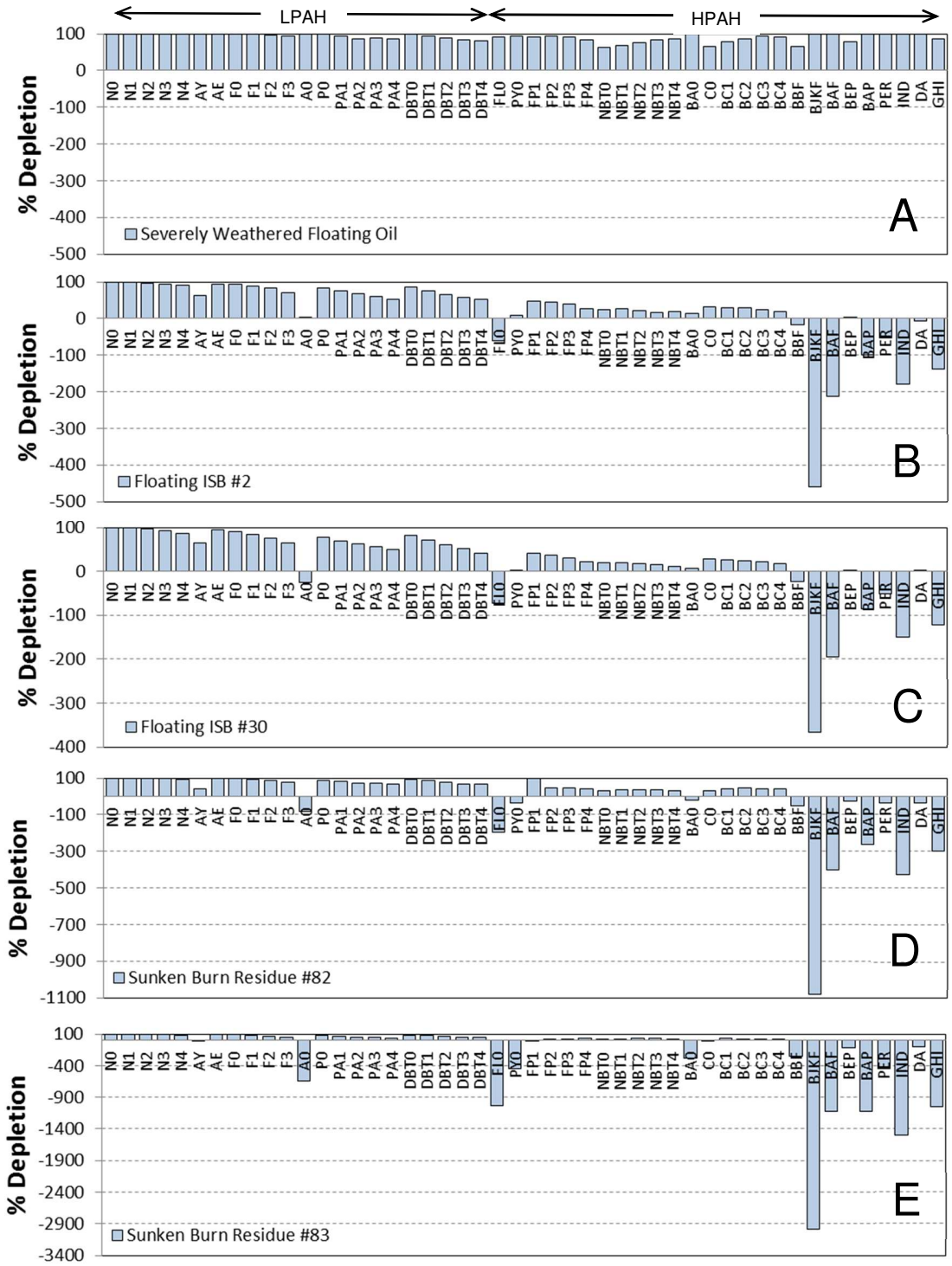

Figure 9: Percent depletions (and enrichments) relative to hopane of individual PAHs for (A) severely (naturally) weathered floating oil, (B) floating ISB residue #2, (C) floating ISB residue #30, (D) sunken ISB residue #82, (E) sunken ISB residue #83, and (E) sunken residue #76. PAH analyte abbreviations from Table 2. Negative percent depletions represent enrichments. Percent depletions calculated from Eq. 1 using data from Table 2. LPAH – lower molecular weight PAHs (2- and 3-rings); HPAH – higher molecular weight PAHs (4- to 6-rings).

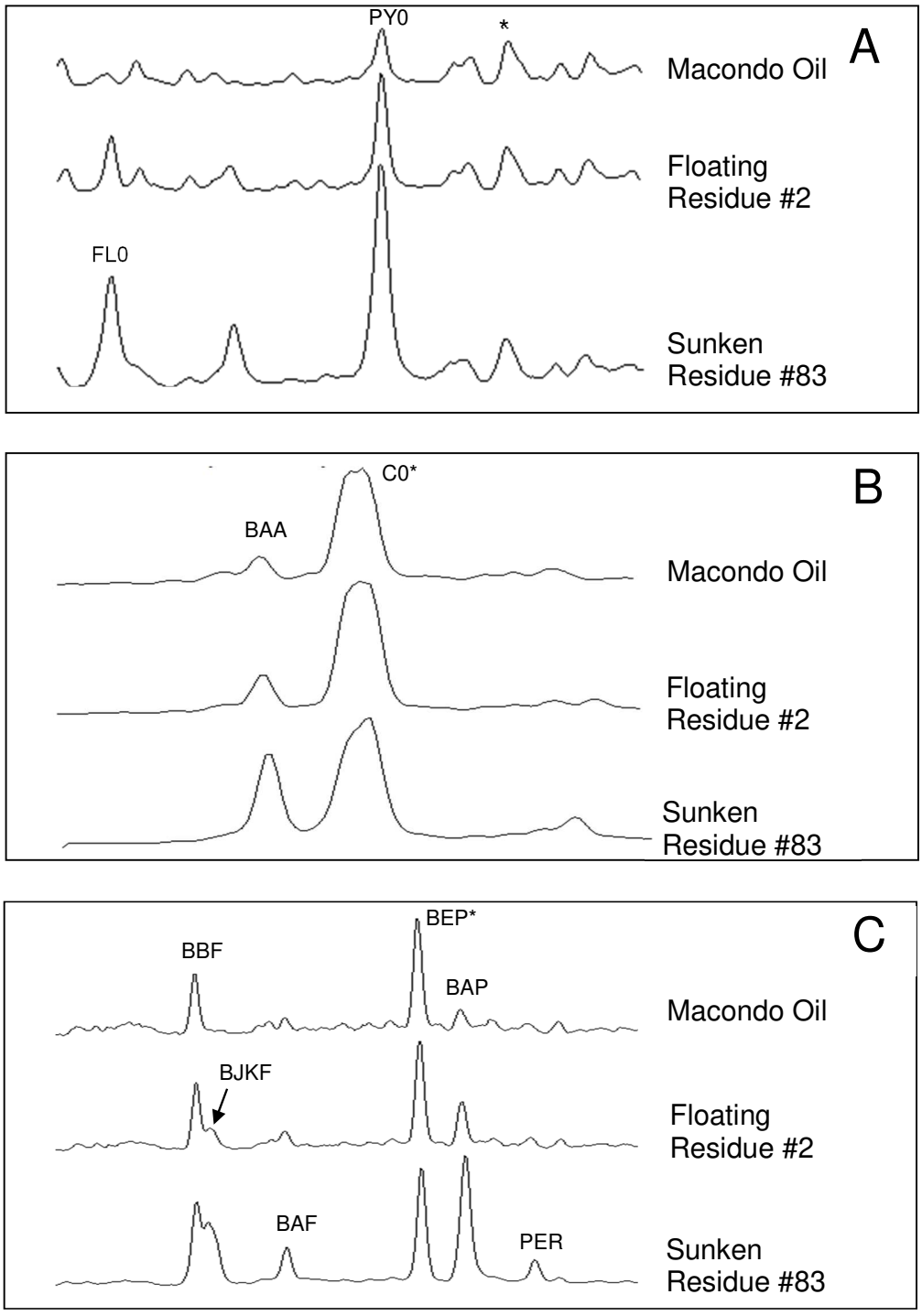

Figure 10: Partial EIPs showing PAH isomer changes in burn residues compared to fresh Macondo oil. (A) fluoranthene and pyrene (*m/z* 202), (B) benz(*a*)anthracene and chrysene (*m/z* 228), and (C) benzofluoranthenes and benzo(*a*)pyrene (*m/z* 252). EIPs normalized to peaks marked with asterisk. Abbreviations from Table 2.

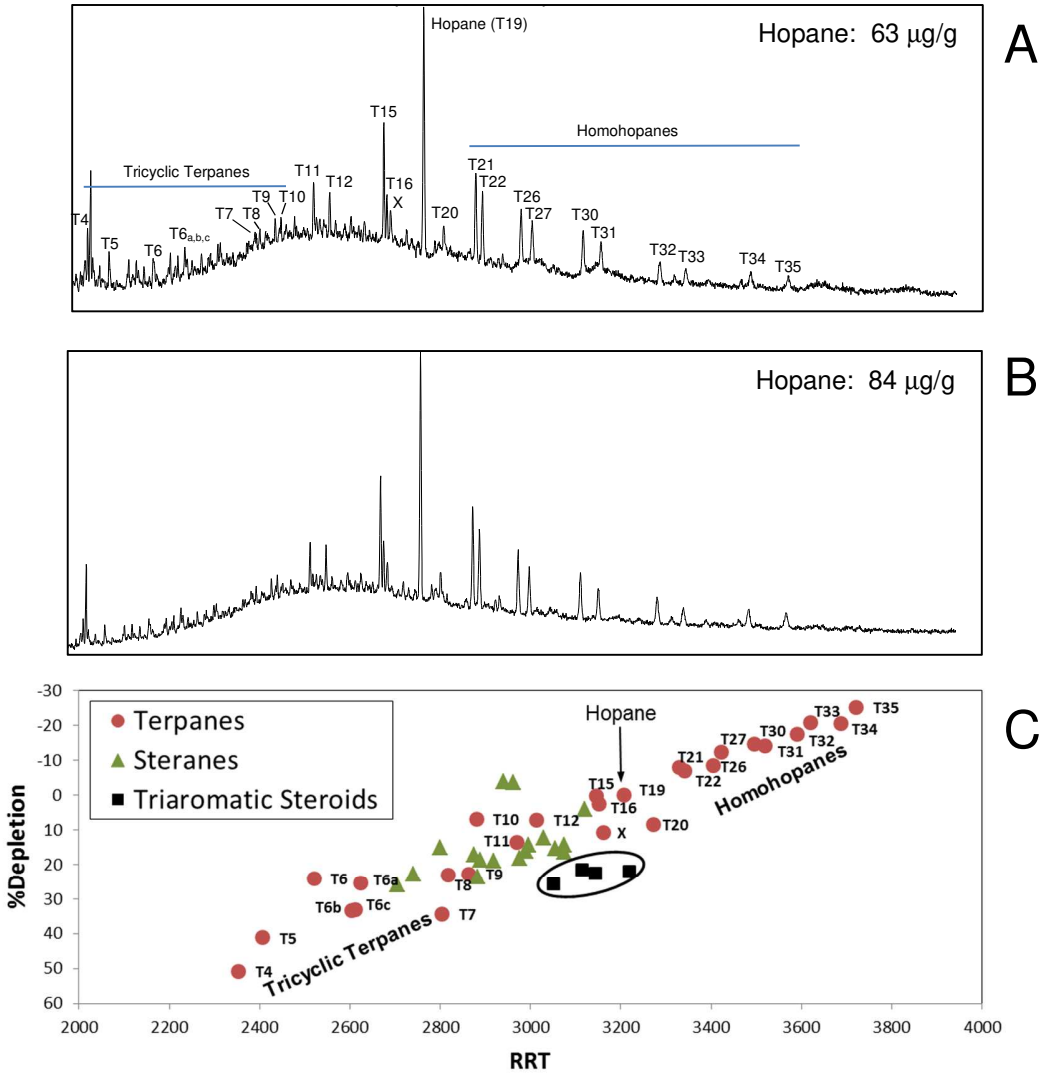

Figure 11: Partial *m/z* 191 EIPs showing distributions of terpanes in (A) fresh Macondo oil and (B) floating in-situ burn residue #2. (C) percent depletion of biomarkers versus relative retention time (RRT) for floating ISB residue #2. RRT in (C) refers to *n*-alkane carbon number, e.g. *n*-C_{20} = 2000, n-C_{30} = 3000, etc. Percent depletions in (C) calculated from Eq. 1 using data from Table 3.

Chemical Composition of Floating and Sunken In-Situ Burn Residues from the Deepwater Horizon Oil Spill

Scott A. Stout[a*] and James R. Payne[b]

[a]NewFields Environmental Forensics Practice, LLC, 300 Ledgewood Pl., Suite 305, Rockland, MA
[b]Payne Environmental Consultants, Inc., 1651 Linda Sue Lane, Encinitas, CA

Graphical Abstract